Inorg. Chem. **2006**, *45*, 8785–8798

Synthesis and Coordination Behavior of Planar-Chiral Ferrocene Alkenylphosphines

Petr Štěpnička* and Ivana Císařová

Department of Inorganic Chemistry, Faculty of Science, Charles University in Prague, Hlavova 2030, 12840 Prague, Czech Republic

Received July 11, 2006

A series of planar-chiral ferrocene alkenylphosphines, (S_p)-2-(diphenylphosphino)-1-vinylferrocene (**2**), (S_p)-2-(diphenylphosphino)-1-(prop-1-en-1-yl)ferrocene (**3**; as a mixture of *Z* and *E* isomers in ca. 5:1 ratio), and (*E*,S_p)-2-(diphenylphosphino)-1-(2-phenylethen-1-yl)ferrocene ((*E*)-**4**), was obtained by Wittig and Horner–Wadsworth–Emmons reactions from the common precursor, (S_p)-2-(diphenylphosphino)ferrocene-1-carboxaldehyde (**1**). Coordination properties of these novel ferrocene donors were studied in their palladium(II) and tungsten(0)–carbonyl complexes. The reaction between **2** and [{Pd(μ-Cl)(L^{NC})}$_2$] (**5**, L^{NC} = 2-{(dimethylamino)methyl-κN}phenyl-κC^1) gave the bridge-cleavage product [PdCl(L^{NC})(**2**-κP)] (**6**) while the reaction with [Pd(L^{NC})(MeCN)$_2$]ClO$_4$ (**7**) yielded the cationic bis(chelate) [Pd(L^{NC})(**2**-η^2:κP)]ClO$_4$ (**8**). Chelate complexes of the type [W(CO)$_4$(L-η^2:κP)] (**9** with L = **2**; (*Z*/*E*)-**10** with L = (*Z*/*E*)-**3**) were obtained by reacting [W(CO)$_4$(cod)] (cod = η^2:η^2-cycloocta-1,5-diene) with the appropriate phosphinoalkene in refluxing toluene while a similar reaction with (*E*)-**4** yielded mixtures of [W(CO)$_5$-(**4**-κP)] ((*E*)-**11**) and [W(CO)$_4$(**4**-η^2:κP)] ((*E*)-**12**). All compounds were characterized by spectral methods (multinuclear NMR, IR, MS, and CD), and the structures of **1**, **2**, **8**, **9**, (*Z*/*E*)-**10**, and (*E*)-**11** were corroborated by X-ray diffraction analysis. Ligands **2** and (*E*)-**4** as well as their complexes **6**, **8**, **9**, (*E*)-**11**, and (*E*)-**12** were further studied by electrochemical methods.

Introduction

Multidentate ferrocene phosphines proved successful as both versatile ligands in the common laboratory praxis and efficient catalyst components at industrial scale.[1] Their chemistry, however, is still strongly dominated by compounds combining the "standard" donor groups, i.e., by ligands of the PP, PN, and PO types; only little attention has been paid to coordination chemistry and catalysis with compounds bearing another *soft* donor group in addition to the phosphine moiety.[1d]

This is particularly the case of ferrocene ligands that combine the usual donor groups with potentially π-donating functionalities such as alkenyl groups that still represent an area remaining largely a virgin field, which markedly contrasts with the number of functionalized vinylferrocenes already known. For instance, racemic vinylferrocenes bearing an additional functional group in position 2 of the ferrocene unit (see Chart 1, structure **A**; Y = Cl, C(O)Ph, C(OH)Ph$_2$, C(O)NHPh) were prepared as early as 1971 by base-induced elimination from the respective (2-ferrocenylethyl)ammonium salts.[2] More recent examples include predominantly synthetic intermediates occurring en route to other ferrocene derivatives. Thus, (S_p)-2-formyl-1-vinylferrocene (**A**, Y = CHO) and its related hydroxymethyl compounds [**A**, Y = CH$_2$OH and CH$_2$OSiMe$_2$(*t*-Bu)] were synthesized and further utilized in the synthesis of conjugated alkenes [**A**; Y = (CH=CH)$_n$(C$_6$H$_4$NO$_2$-4), n = 1−3] with an aim of preparing new materials for nonlinear optics.[3] Pyridyl-substituted vinylferrocenes (**A**, Y = 2-chloropyrid-3-yl and 2-vinylpyrid-3-yl) were used as precursors to ferroceno-fused (iso)-quinolines,[4] while (S_p)-1-vinylferrocene-2-carboxylic acid (**A**,

* To whom correspondence should be addressed. E-mail: stepnic@natur.cuni.cz.

(1) (a) *Ferrocenes-Homogeneous Catalysis, Organic Synthesis, Materials Science*; Togni, A., Hayashi, T., Eds.; VCH: Weinheim, Germany, 1995. (b) Togni, A. *New Chiral Ferrocenyl Ligands for Asymmetric Catalysis* in *Metallocenes-Synthesis, Reactivity, Applications*; Togni, A., Halterman, R. L., Eds.; Wiley-VCH: Weinheim, Germany, 1998; Vol. 2, Chapter 11, pp 685−721. (c) Colacot, T. J. *Chem. Rev.* **2003**, *103*, 3101−3118. (d) Atkinson, R. C. J.; Gibson, V. C.; Long, N. J. *Chem. Soc. Rev.* **2004**, *33*, 313−328.

(2) Slocum, D. W.; Jennings, C. A.; Engelmann, T. R.; Rockett, B. W.; Hauser, C. R. *J. Org. Chem.* **1971**, *36*, 377−381.

(3) Togni, A.; Rihs, G. *Organometallics* **1993**, *12*, 3368−3372.

(4) Mamane, V.; Fort, Y. *J. Org. Chem.* **2005**, *70*, 8220−8223.

10.1021/ic061278g CCC: $33.50
Published on Web 08/30/2006

Chart 1

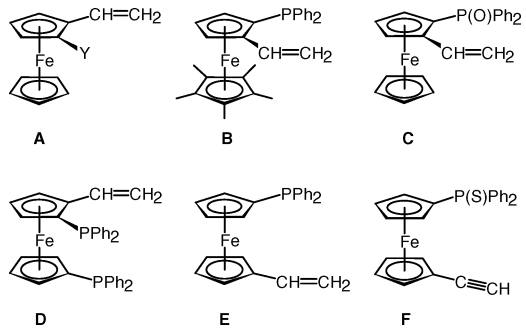

Y = CO_2H) and its carbamate (**A**, Y = $NHC(O)OCH_2Ph$) represent the key intermediates in the synthesis of chiral phosphinoamine and amidinato ligands.[5] Finally, N-substituted amides of (R_p)-1-vinylferrocene-2-carboxylic acid that are accessible by sparteine-mediated diastereoselective *ortho*-metalation of $FcC(O)NEt(CMe_2Ph)$ followed by vinylation of carboxaldehyde intermediates [**A**, Y = C(O)NHR and $C(O)NR_2$] were further converted to planar-chiral, phosphino-substituted ferrocene lactones.[6] Yet another example in which two potentially π-donating groups are combined is 2-ethinyl-1-vinylferrocene (**A**, Y = C≡CH).[7]

Phosphorus-substituted vinylferrocenes, which were not mentioned in the above list, were also synthesized either unintentionally or served just as reaction intermediates. The representative examples are (R_p)-2-(diphenylphosphino)-1′,2′,3′,4′,5′-pentamethyl-1-vinylferrocene (Chart 1, **B**), which was obtained from heating (S,R_p)-2-(diphenylphosphino)-1′,2′,3′,4′,5′-pentamethyl-1-(1-(dimethylamino)ethyl)ferrocene with acetic anhydride,[8] and (R_p)-2-(diphenylphosphinoyl)-1-vinylferrocene (Chart 1, **C**), which served as a precursor to planar-only chiral (R_p)-1-diphenylphosphino-2-ethylferrocene.[9] The related diphosphine, 2,1′-bis(diphenylphosphino)-1-vinylferrocene (Chart 1, **D**), is also known and was employed in the preparation of polymer-supported palladium catalyst.[10] However, there has been as yet no systematic investigation into the donor properties of these potentially interesting molecules.

We have recently reported about the synthesis and coordination behavior of 1′-(diphenylphosphino)-1-vinylferrocene (Chart 1, **E**)[11] and the related alkynyl−phosphine sulfide, 1′-(diphenylthiophosphoryl)-1-ethynylferrocene (Chart 1, **F**).[12] As a next step in exploring the chemistry of ferrocene-based P/π-donors, we turned—in view of the well-established chemistry of *ortho*-alkenyl-substituted triphenylphosphines[13]—to planar-chiral 2-(diphenylphosphino)-1-alkenylferrocenes. In this contribution we report about the preparation of several enantiopure phosphinoferrocenes substituted by various alkenyl groups and their coordination behavior in palladium(II) and tungsten−carbonyl complexes. We also describe the solid-state structures and electrochemical properties of the obtained compounds.

Results and Discussion

Preparation and Structural Characterization of the Ligands.[14] Vinyl phosphine **2**[15] was synthesized by Wittig vinylation from (S_p)-2-(diphenylphosphino)-1-ferrocenecarboxaldehyde[16] (**1**; Scheme 1). Purification by column chromatography followed by crystallization from heptane afforded the compound as an air-stable, rusty brown crystalline solid in a very good yield.

(5) Bertogg, A.; Togni, A. *Organometallics* **2006**, *25*, 622−630.
(6) Metallinos, C.; Szillat, H.; Taylor, N. J.; Snieckus, V. *Adv. Synth. Catal.* **2003**, *345*, 370−382.
(7) (a) Bunz, U. H. F. *J. Organomet. Chem.* **1995**, *494*, C8−C11. Examples of FcCH=CHR alkenes (R = Me or Ph) substituted in position 2 of the ferrocene unit are even less common. See, e.g.: (b) Toma, Š.; Kaluzayova, E. *Chem. Zvesti* **1969**, *23*, 540−552. (c) Benedikt, M.; Schlögl, K. *Monatsh. Chem.* **1978**, *109*, 805−822. (d) Izumi, T.; Endo, K.; Saito, O.; Shimizu, I.; Maemura, M.; Kasahara, A. *Bull. Chem. Soc. Jpn.* **1978**, *51*, 663−664.
(8) Abbenhuis, H. C. L.; Burckhardt, U.; Gramlich, V.; Togni, A.; Albinati, A.; Müller, B. *Organometallics* **1994**, *13*, 4481−4493.
(9) Hayashi, T.; Mise, T.; Fukushima, M.; Kagotani, M.; Nagashima, N.; Hamada, Y.; Matsumoto, A.; Kawakami, S.; Konishi, M.; Yamamoto, K.; Kumada, M. *Bull. Chem. Soc. Jpn.* **1980**, *53*, 1138−1151.
(10) (a) Stille, J. K.; Su, H.; Hill, D. H.; Schneider, P.; Tanaka, M.; Morrison, D. L.; Hegedus, L. S. *Organometallics* **1991**, *10*, 1993−2000. This diphosphine was also obtained a side product from the attempted synthesis of a chiral, azacrown-substituted ferrocenyldiphosphine: (b) Landis, C. R.; Sawyer, R. A.; Somsook, E. *Organometallics* **2000**, *19*, 994−1002. A related 1,1′-bis(alkenyl)-2,2′-diphosphine as a precursor for chiral ferrocene diphosphine can be found in: (c) Kang, J.; Lee, J. H.; Choi, J. S. *Tetrahedron: Asymmetry* **2001**, *12*, 33−35.
(11) Štěpnička, P.; Císařová, I. *Collect. Czech. Chem. Commun.* **2006**, *71*, 215−236.
(12) Štěpnička, P.; Císařová, I. *J. Organomet. Chem.* **2006**, *691*, 2863−2871.
(13) Selected examples are as follows. (2-$Ph_2PC_6H_4$)CH=CH_2 (**I**): (a) Bennett, M. A.; Nyholm, R. S.; Saxby, J. D. *J. Organomet. Chem.* **1967**, *10*, 301−306. (b) Brookes, P. R. *J. Organomet. Chem.* **1972**, *42*, 459−469. (c) Robertson, G. B.; Whimp, P. O. *J. Chem. Soc., Dalton Trans.* **1973**, 2454−2459. (d) Bennett, M. A.; Johnson, R. N., Tomkins, I. B. *J. Am. Chem. Soc.* **1974**, *96*, 61−69. (e) Bennett, M. A.; Johnson, R. N.; Tomkins, I. B. *Inorg.* Chem. **1974**, *13*, 346−350. (f) Bennett, M. A.; Hann, E. J.; Jonson, R. N. *J. Organomet. Chem.* **1977**, *124*, 189−211. (g) Bennett, M. A.; Chee, H.-K.; Jeffery, J. C.; Robertson, G. B. *Inorg. Chem.* **1979**, *18*, 1071−1076. (h) Bruce, M. I.; Hambley, T. W.; Snow, M. R.; Swincer, A. G. *J. Organomet. Chem.* **1984**, *273*, 361−376 and references therein. (i) Bruce, M. I.; Williams, M. L. *J. Organomet. Chem.* **1986**, *314*, 323−331. (j) Bennett, M. A.; Chiraratvatana, C.; Robertson, G. B. *Organometallics* **1988**, *7*, 1394−1402. (k) Bennett, M. A.; Chiraratvatana, C.; Robertson, G. B.; Tooptakong, U. *Organometallics* **1988**, *7*, 1403−1409. (l) Cavell, K. J.; Hong, J. *J. Chem. Soc., Dalton Trans.* **1995**, 4081−4089. (m) Parish, R. V.; Boyer, P.; Fowler, A.; Kahn, T. A.; Cross, W. I.; Pritchard, R. G. *J. Chem. Soc., Dalton Trans.* **2000**, 2287−2294. (2-$Ph_2PC_6H_4$)CH_2CH=CH_2 (**II**): (n) Interrante, L. V.; Bennett, M. A.; Nyholm, R. S. *Inorg. Chem.* **1966**, *5*, 2212−2217. (o) Bennett, M. A.; Kneen, W. R.; Nyholm, R. S. *Inorg. Chem.* **1968**, *7*, 556−560. **I** and **II**: (p) Bennett, M. A.; Kneen, W. R., Nyholm, R. S. *J. Organomet. Chem.* **1971**, *26*, 293−303. **I**, (2-$Ph_2PC_6H_4$)CH=CHMe, and **II**: (q) Interrante, L. V.; Nelson, G. V. *Inorg. Chem.* **1968**, *7*, 2059−2064. **II** and (2-$Ph_2PC_6H_4$)CH(Me)CH=CH_2: (r) Bennett, M. A.; Kneen, W. R.; Nyholm, R. S. *Inorg. Chem.* **1968**, *7*, 552−556. (2-$Ph_2PC_6H_4$)$(CH_2)_3$CH=CH_2: (s) Bennett, M. A.; Kouwenhoven, H. W.; Lewis, J.; Nyholm, R. S. *J. Chem. Soc.* **1964**, 4570−4577. P(C_6H_4-CH=CH_2-2)$_3$ and PhP(C_6H_4CH=CH_2-2)$_2$: (t) Hall, D. I.; Nyholm, R. S. *J. Chem. Soc., Chem. Commun.* **1970**, 488−4879. (u) Nyholm, R. S.; Hall, D. I. *J. Chem. Soc. A* **1971**, 1491−1493. (v) Hall, D. I.; Nyholm, R. S. *J. Chem. Soc., Dalton Trans.* **1972**, 804−809. **I** and (2-$Ph_2PC_6H_4$)CH=CHPh: (w) Bennett, M. A.; Kapoor, P. N. *J. Organomet. Chem.* **1987**, *336*, 257−269. $Ph_2PCH_2SiMe_2(CH$=$CH_2)$: (x) Alyea, E. C.; Meehan, P. R.; Ferguson, G.; Kannan, S. *Polyhedron* **1997**, *16*, 3479−3481.
(14) Since all compounds are (S_p)-chiral, the descriptor specifying chirality at the 1,2-disubstituted cyclopentadienyl plane is omitted for clarity.
(15) The isomer (R_p)-**2** has been already mentioned in the literature as a side product from diastereoselective synthesis of tetracyclic precursors to vinblastine using (S,R_p)-1-[2-(diphenylphosphino)ferrocenyl]ethyl acetate as a chiral auxiliary. For reference, see: Kuehne, M. E.; Bandarage, U. K. *J. Org. Chem.* **1996**, *61*, 1175−1179.
(16) (a) Riant, O.; Samuel, O.; Kagan, H. B. *J. Am. Chem. Soc.* **1993**, *115*, 5835−5836. (b) Riant, O.; Samuel, O.; Flessner, T.; Taudien, S.; Kagan, H. B. *J. Org. Chem.* **1997**, *62*, 6733−6745.

Scheme 1. Preparation of the Ligands

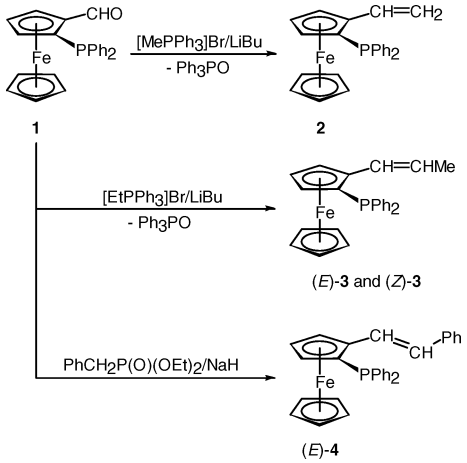

The prop-1-en-1-yl analogue, compound **3**, was prepared similarly. In this case, however, the Wittig reaction with the in situ generated ylide $Ph_3P{=}CHMe$ afforded a mixture of double-bond configurational isomers with the *Z*-isomer dominating (the (*Z*)-**3**:(*E*)-**3** ratio as determined by NMR was ca. 5:1). This isomer ratio is in accordance with the stereochemical outcome usually observed for reactions with triphenylphosphine-based Wittig reagents[17,18] which, in turn, indicates that the proximal phosphino group represents no pronounced stereochemical bias for the course the alkenylation reactions involving aldehyde **1**. Attempts to separate the isomers by chromatography or crystallization failed due to their similar solubility and retention characteristics. To circumvent similar difficulties with isomer separation, the 2-phenyleth-1-en-1-yl derivative was prepared by Horner−Wadsworth−Emmons reaction (HWE)[18,19] (Scheme 1). Again, in agreement with the stereoselectivity of the HWE olefination,[18] the respective phosphinoalkene **4** was isolated exclusively as the *E*-isomer after chromatography and crystallization from heptane.

Phosphinoalkenes **2**−**4** were characterized by the standard analytical methods, and the solid-state structures of **1** and **2** were determined by single-crystal X-ray diffraction. The formulation of **2**−**4** is in accordance with their spectral and analytical data. In ^1H and ^{13}C NMR spectra, the compounds exhibit characteristic signals due to 1,2-disubstituted ferrocene framework and vinyl group (**2**) or 1,2-disubstituted double bonds ((*Z*/*E*)-**3** and (*E*)-**4**). The phosphine substituents give rise to signals at $\delta_P \approx -21$ in ^{31}P NMR spectra.

The solid-state structures of **1** and **2** are shown in Figures 1 and 2, respectively, along with the relevant structural parameters. The structures fully corroborate the expected ones including absolute configuration at the disubstituted cyclopentadienyl plane. The geometry of the (diphenylphosphino)ferrocenyl moieties in both compounds is very similar and quite regular. In both cases, the carbon substituents

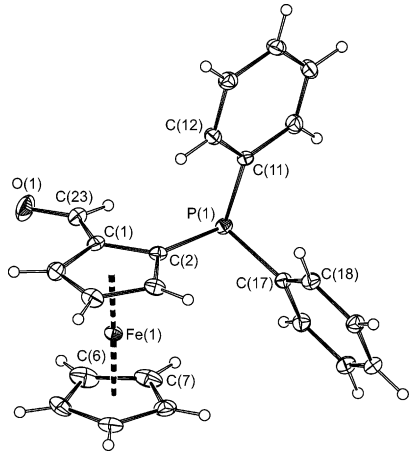

Figure 1. View of molecule 1 in the crystal structure of **1** showing displacement ellipsoids at the 30% probability level. Selected geometric parameters for molecule 1 [molecule 2]: C(1)−C(23) 1.455(3) [C(31)−C(53) 1.463(2)], C(23)−O(1) 1.215(3) [C(53)−O(2) 1.219(2)], P(1)−C(2) 1.821(2) [P(2)−C(32) 1.817(2)], P(1)−C(11) 1.840(2) [P(2)−C(41) 1.836-(2)], P(1)−C(17) 1.836(2) [P(2)−C(47) 1.835(2)] Å; C(2)−C(1)−C(23) 125.7(2) [C(32)−C(31)−C(53) 125.8(2)], C(1)−C(23)−O(1) 125.0(2) [C(31)−C(53)−O(2) 123.4(1)]°; torsion angles C(23)−C(1)−C(2)−P(1) 7.1(3) [C(53)−C(31)−C(32)−P(2) 14.9(2)]°.

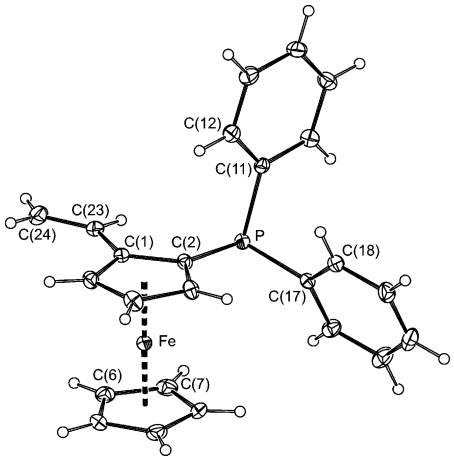

Figure 2. The molecular structure of (S_p)-**2**. Displacement ellipsoids are shown at the 30% probability level. Selected geometric parameters: C(1)−C(23) 1.463(2), C(23)−C(24) 1.323(3), P−C(2) 1.817(2), P−C(11) 1.838-(2), P−C(17) 1.837(2) Å; C(2)−C(1)−C(23) 125.6(2), C(1)−C(23)−C(24) 126.4(2), P−C(2)−C(1) 123.5(1), C−P−C angles 98.68(7)−102.30(7)°; torsion angle C(23)−C(1)−C(2)−P −3.4(2)°; ferrocene unit Fe−Cg(1) 1.6478(7), Fe−Cg(2) 1.6596(8) Å, ∠Cp(1),Cp(2) 1.9(1)°. Definitions: Cp-(1) [Cp(2)] are the cyclopentadienyl rings C(1−5) [C(6−10)]; Cg(1,2) denote their respective centroids.

(aldehyde or vinyl group) are directed outward the phosphino substituent while remaining nearly parallel with their parent cyclopentadienyl ring, thus allowing for an efficient conjugation. This can be demonstrated by the angles subtended by the C=O or C=C bonds and the Cp1 planes of 0.6(2)° for molecule 1 [3.2(1)° for molecule 2] in **1** and 7.4(2)° in **2**, and further by the torsion angles C(2)−C(1)−C(23)−O(1) −179.6(2)° [C(32)−C(32)−C(53)−O(2) 175.5(2)°] for the aldehyde and C(2)−C(1)−C(23)−C(24) of −171.1(2)° for **2**. Bond lengths within the carbon substituents are similar to those in respectively $Ph_2PfcCHO$ (fc = ferrocene-1,1′-diyl; C=O 1.213(4) Å)[20] and $Ph_2P(S)fcCH{=}CH_2$ (C=C 1.314(3) Å)[11] or 1′,1‴-divinylbiferrocene (C=C 1.300(7) Å).[21]

(17) Wittig, G.; Schöllkopf, U. *Chem. Ber.* **1954**, *87*, 1318−1330 and references therein.
(18) Maryanoff, B. E.; Reitz, A. B. *Chem. Rev.* **1989**, *89*, 863−927.
(19) (a) Horner, L.; Hoffmann, H.; Wippel, J. H. G.; Klahre, G. *Chem. Ber.* **1959**, *92*, 2499−2505. (b) Wadsworth, W. S., Jr.; Emmons, W. D. *J. Am. Chem. Soc.* **1961**, *83*, 1733−1738. (c) Wadsworth, W. S., Jr. *Org. React.* **1977**, *25*, 73−253.

Scheme 2

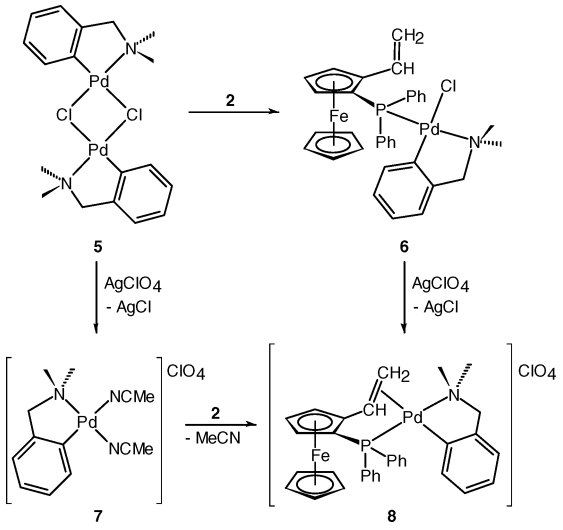

Palladium Complexes with Ligand 2. The donor ability of the simplest representative **2** was first studied in reactions with palladium(II) complexes bearing *ortho*-metalated *N*,*N*-benzylamine as a supporting ligand. Quite expectedly, cleavage of halide bridges in the dinuclear complex **5** gave complex **6** featuring **2** as a *P*-monodentate phosphine. Chelate coordination was achieved upon changing the palladium precursor to the cationic bis(acetonitrile) complex **7**[22] or, alternatively, by halide removal from **6** with silver(I) perchlorate (Scheme 2).

The coordination of **2** via the phosphorus atom is clearly manifested by low-field ^{31}P NMR shifts (cf. the coordination shifts, $\Delta = \delta$(complex) $- \delta$(ligand), Δ_P(**6**) $= +52.7$ and Δ_P(**8**) $= +51.3$). On the contrary, the interaction between the ligand vinyl moiety and the palladium center is difficult to decide on from NMR spectra only since they exhibit no significant changes for the double bond resonances. For instance, the ^{13}C NMR signals of the vinyl groups in **2**, **6**, and **8** are found in narrow ranges of 100.93−112.36 (=CH_2) and 132.24−134.15 (=CH) (cf. the data for the tungsten complexes below). The ferrocene signals are little informative also [see, e.g., δ_C for the phosphine/vinyl-bearing cyclopentadienyl carbon atoms: 75.89/88.79 (**2**), 72.41/87.76 (**6**), and n.o./90.25 (**8**)]. Likewise, the NMR signals due to the 2-{(dimethylamino)methyl}phenyl (L^{NC}) ligands in **6** and **8** are observed at similar positions but with differences between chemical shifts of the diastereotopic NCH_2 and NMe_2 protons larger in **8** that in **6** (**6**/**8**: $\Delta\delta$(NCH_2) 0.04/0.43, $\Delta\delta$(NMe_2) 0.20/0.95). The $^4J_{PH}$ and $^3J_{PC}$ coupling constants for the NCH_2 and NMe_2 groups[22,23] allow one to formulate complexes **6** and **8** as having *trans*-P−N geometry. ESI mass spectra of **6** and **8** show prominent ions at *m*/*z* 636 attributable to [Pd(L^{NC})(**2**)]$^+$ formed by either loss of chloride (**6**) or dissociation (**8**).

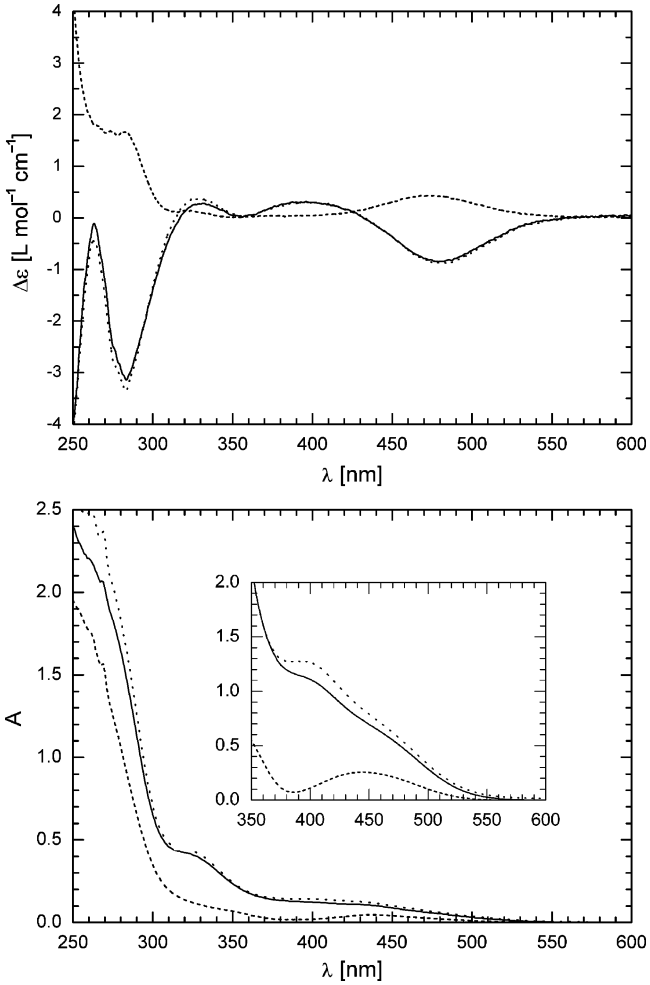

Figure 3. CD (top) and UV−vis spectra (bottom, 1 mm optical path) of ligand **2** (dashed line) and its palladium(II) complexes **6** (solid line) and **8** (dotted line). For the latter case, the inset shows an expansion of the long-wavelength region (1 cm optical path; i.e., 10-fold in the *A*-axis). The spectra were recorded in methanol (1 mM solutions and 1 cm/1 mm optical paths for the UV−vis spectra; roughly similar but varying concentrations for individual compounds for the CD spectra).

CD spectra of free ligand **2** are strikingly different from those of its palladium complexes **6** and **8** (Figure 3). At first sight, the spectra could have been interpreted as belonging to compounds with the opposite configuration at the stereogenic element (see, e.g., opposite signs of the Cotton effect at around 475 nm). However, since the CD spectra reflect the *same* planar chirality at the ferrocene unit, the reason for the different response should be sought in the shift of the electronic absorption bands upon coordination. This assumption is supported by UV−vis spectra (Figure 3), which are very similar for both palladium complexes but differ markedly from that of **2**.[24] The presented results clearly indicate that CD spectra of similar systems should be interpreted with caution to avoid confusing conclusions.

The crystal structure of **8** was determined by X-ray diffraction analysis. The molecular structure of the cation

(20) Štěpnička, P.; Baše, T. *Inorg. Chem. Commun.* **2001**, *4*, 682−687.
(21) Dong, T.-Y.; Hwang, M.-Y.; Hsu, T.-L.; Schei, C.-C.; Yeh, S.-K. *Inorg. Chem.* **1990**, *29*, 80−84.
(22) Štěpnička, P.; Lamač, M.; Císařová, I. *Polyhedron* **2004**, *23*, 921−928.
(23) Štěpnička, P.; Císařová, I. *Organometallics* **2003**, *22*, 1728−1740.

(24) The similarity of the UV−vis and CD spectra of **6** and **8** may also suggest similar species to be involved, formed by dissociation of **6** (at least partial) in the polar solvent (methanol). This explanation cannot be simply ruled out albeit NMR data ($\Delta_P = 52.7$ in CD_3OD) stand against it.

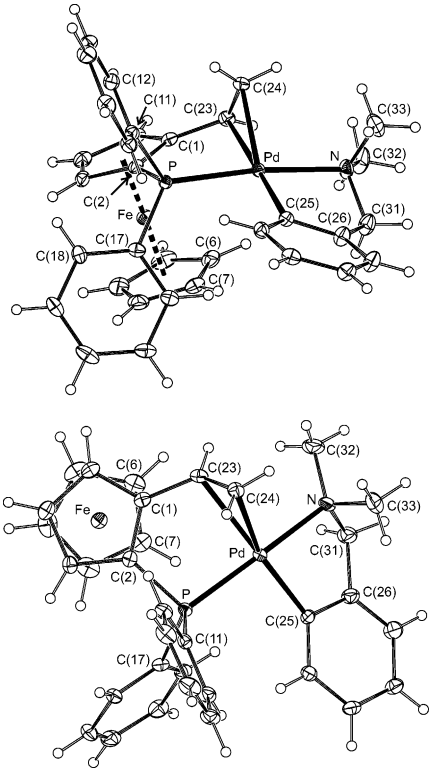

Figure 4. Side (top) and top (bottom) views with respect to the coordination plane of the complex cation $[Pd(L^{NC})(\mathbf{2}\text{-}\eta^2{:}\kappa P)]^+$ in **8**. Displacement ellipsoids are shown with 30% probability.

Table 1. Selected Interatomic Distances (Å) and Angles (deg) for **8**[a,b]

Pd−P	2.2729(6)	P−C(2)	1.794(3)
Pd−N	2.150(2)	P−C(11)	1.823(3)
Pd−Cg(3)	2.307(3)	P−C(17)	1.818(3)
Pd−C(23)	2.477(3)	N−C(31)	1.481(5)
Pd−C(24)	2.324(3)	N−C(32)	1.458(4)
Pd−C(25)	2.022(3)	N−C(33)	1.502(4)
C(23)−C(24)	1.340(4)	C(26)−C(31)	1.498(4)
C(1)−C(23)	1.470(4)		
P−Pd−Cg(3)	87.89(8)	C(1)−C(23)−C(24)	123.3(2)
P−Pd−C(25)	96.54(7)	C(2)−C(1)−C(23)	125.0(2)
N−Pd−Cg(3)	95.1(1)	C(5)−C(1)−C(23)	127.6(2)
N−Pd−C(25)	81.6(1)	C(1)−C(2)−P	120.2(2)
N−C(31)−C(26)	108.4(3)	C(3)−C(2)−P	131.9(2)
C(23)−Pd−C(25)	173.71(9)	C(24)−Pd−C(25)	153.4(1)
Fe−Cg(1)	1.641(1)	∠Cp(1),Cp(2)	4.5(2)
Fe−Cg(2)	1.654(2)		

[a] Definitions are as follows. Ring planes: Cp(1), C(1−5); Cp(2), C(6−10); Cg(1) and Cg(2) are the respective ring centroids. Cg(3) denotes the midpoint of the η^2-coordinated double bond C(23)═C(24). [b] Structural data for the perchlorate counterion: Cl−O(1) 1.439(3), Cl−O(2) 1.445(3), Cl−O(3) 1.428(3), Cl−O(4) 1.440(3) Å; O−Cl−O angles 108.9(2)−110.1(2)°.

in the structure of **8** is shown in Figure 4, and the selected structural data are given in Table 1. The structure confirms the expected chelate coordination of the phosphinoalkene as well as the *trans*-P−N disposition of the donors. To describe the coordination geometry, we take the midpoint of the η^2-double bond (or Cg(3)) as the ligating site. Then, the interligand angles span the range 81.6(1)−96.54(7)° with the angles within both chelate rings being more acute that the remaining ones. The Pd−X bonds length (X = P, N, and C(25)) as well as the geometry of the five-membered palladacycle compare favorably with those observed for related, structurally characterized complexes featuring other ferrocene phosphines.[22,23] As indicated by the ring-puckering parameters[25] (Q_2 = 0.442(3) Å, ϕ_2 = 222.7(4)°), the palladacycle adopts an envelope conformation. The phenyl ring C(25−30) which is a part of the cycle is rotated from the plane comprising the Pd, P, N, and C(25) atoms (PdL_3) by 19.8(1)°.

Structurally more interesting features can be seen within phosphinoalkene part, where steric strain imposed by the chelate coordination leads to deformation of both the coordination sphere around palladium(II) and the ligand molecule. The η^2-coordinated double bond is tilted with respect to the PdL_3 plane at an angle of 69.8(2)°, and consequently, the C(23)−Pd−C(25) and C(24)−Pd−C(25) angles differ by as much as 20°. In addition, the double bond coordinates to the palladium atom somewhat asymmetrically: the Pd−C(23,24) bond lengths differ by about 0.15 Å and the center of the double bond (or Cg(3)) is shifted with respect to the projection of the Pd−C(25) bond in the trans position. Notably, the coordination causes only a negligible elongation of the double bond (by only ca. 1% with respect to uncoordinated **2**). Indeed, this is in accordance with the NMR data but contrasts with the structure of $[Pd\{(2\text{-}Ph_2PC_6H_4)CH{=}CH_2\text{-}\eta^2{:}\kappa P\}\{(2\text{-}Ph_2PC_6H_4)CH{=}CH_2\text{-}\kappa P\}]$, where the difference between the coordinated and free double bond lengths amounts to 0.094 Å (or relatively 7%).[13k,26]

The coordination further changes the conformation of the ligand. The C(23)−C(24) bond in **8** is rotated respect to the Cp1 plane at an angle of 43.1(2)° (compare the torsion angle C(2)−C(1)−C(23)−C(24) = −52.5(4)° with that in uncoordinated **2**), and simultaneously, the whole vinylphosphine moiety becomes more compact via closure of the C(1)−C(23)−C(24) and C(1)−C(2)−P angles (both by ca. 3°). The C(23) atom binds symmetrically to the Cp1 ring, but the C(2)−P bond is inclined toward the vinyl moiety: whereas the difference of the C(2,5)−C(1)−C(23) angles is below 3°, that between C(3,1)−C(2)−P approaches 12°. In addition, the donor atoms are bent from their parent cyclopentadienyl plane (the perpendicular distances for the P and C(23) atoms to the Cp1 plane are respectively 0.194(1) and 0.117(4) Å) though without significant torsion at the C(1)−C(2) bond (torsion angle C(23)−C(1)−C(2)−P is −4.8(4)°). The whole ferrocene unit is rotated with respect to the PdL_3 plane as exemplified by the dihedral angle 27.5(2)° between the PdL_3 and Cp1 planes.

Preparation and Structures of Tungsten(0) Carbonyls Complexes with 2−4. The reaction between equimolar amounts of **2** and $[W(cod)(CO)_4]$ (cod = $\eta{:}^2\eta^2$-cycloocta-

(25) Cremer, D.; Pople, J. A. *J. Am. Chem. Soc.* **1975**, *97*, 1354−1358. Ideal envelope conformation requires ϕ_2 = 216°. N.B. The ring puckering parameters should be considered informative only because of the different bond lengths within the metallacycle.

(26) A closer look at the geometry of Pd(η^2-RCH═CH_2) moieties in the Cambridge Structural Database (CSD; 35 structures) revealed that there is no pronounced correlation between the coordination distance (Pd−Cg) and the C═C bond length. This is probably because an influence of the double bond substituent (R) on the double bond length is comparable with that of coordination. Nevertheless, the bond lengths observed for **8** are in accordance with mean values from CSD. Source: Cambridge Structural Database version 5.27 of Nov 2005 with updates of Jan 2006.

Scheme 3

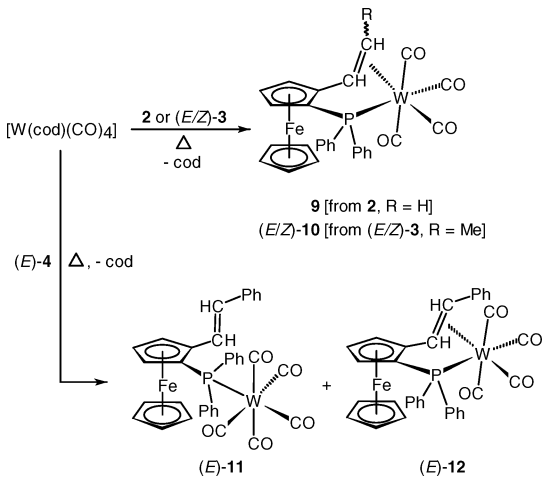

1,5-diene) in refluxing toluene gave air-stable, crystalline complex [W(CO)$_4$(**2**)] (**9**) in 91% isolated yield (Scheme 3).[27] The bidentate coordination of the phosphinoalkene (η^2:κP) in **9** was clearly inferred from NMR spectra and further corroborated by single-crystal X-ray diffraction. In ^{1}H and ^{13}C NMR spectra, the coordination is reflected mainly by a considerable high-field shift of the double bond resonances, the respective values being Δ_H(=CH) = 0.55, Δ_C(=CH$_2$) = 47.8, and Δ_C(=CH) = 51.3. By contrast, the phosphine resonance appears at a significantly lower field (Δ_P = 45.0) flanked with ^{183}W satellites ($^1J_{WP}$ = 249 Hz).[28] In IR spectra, complex **9** shows characteristic strong carbonyl stretching bands: a sharp band at 2022 cm^{-1} and broad, composite bands at around 1920 and 1870 cm^{-1}.

Replacing **2** with (*Z*/*E*)-**3** in the above reaction leads to a mixture of analogous chelate complexes, (*Z*/*E*)-**10** (Scheme 3). Again, the isomers cannot be separated by conventional methods because of their similar rentention and solubility properties (see the crystal structure below). NMR spectra of the reaction mixture recorded prior to chromatography or crystallization indicate that the complexation reaction leaves the original isomer ratio unaltered.

A similar reaction between (*E*)-**4** and [W(cod)(CO)$_4$] is more complicated, giving mixtures of two major products (*E*)-**11** and (*E*)-**12** that differ by the coordination of the phosphinoalkene and the number of ancillary carbonyl ligands (Scheme 3). It is noteworthy that the product ratio changes upon varying the reaction conditions. As expected, higher temperatures and extended reaction times favor the chelate complex (*E*)-**12** while the formation of complex (*E*)-**11** requiring one CO molecule from the "reaction environment"[29] is clearly facilitated at lower temperatures and under stationary conditions (i.e., when no or only moderate refluxing is maintained under static atmosphere and with limited stirring). Compounds (*E*)-**11** and (*E*)-**12** were separated by column chromatography on silica gel. The former, faster eluting complex was isolated as an orange solid which was subsequently crystallized from heptane to yield (*E*)-**11** as well-developed, red crystals, while the *slightly* more polar (*E*)-**12** was obtained in the form of an orange-yellow foam possessing a strong tendency to adsorb reaction solvents.

The complexes could be clearly distinguished on the basis of elemental analyses and NMR and IR spectra. Besides, the structure of (*E*)-**11** was independently corroborated by X-ray diffraction analysis. In ^{1}H and ^{13}C NMR spectra, complex (*E*)-**11** shows the CH=CH resonances within the usual double bond region (δ_C 124.74 and 128.32),[30] while the spectra of its chelate counterpart (*E*)-**12** display the same signals at significantly higher fields (cf. δ_C 75.38 and 86.53). The ^{13}C NMR spectra are also indicative of the carbonyl-substitution pattern: compound (*E*)-**11** exerts a pair of doublets due to four cis (δ_C 197.73, $^2J_{PC}$ = 7 Hz) and one trans (δ_C 198.97, $^2J_{PC}$ = 22 Hz) tungsten-bonded carbonyl ligands, while (*E*)-**12** shows four well-separated, phosphorus-coupled doublets with characteristic ^{183}W satellites between δ_P ca. 201 and 213 in a pattern similar to that for **9**. The coordination shift observed in ^{31}P NMR spectra for chelate complex (*E*)-**12** (Δ_P = 46.6, $^1J_{WP}$ = 293 Hz) is much larger than for (*E*)-**11** (Δ_P = 32.8, $^1J_{WP}$ = 246 Hz), which is in accordance with bidentate coordination of (*E*)-**4** in the former case. The observed shifts are significantly larger than those observed in [W(CO)$_5$(dppf-κP)], [(μ-dppf-1κP,2$\kappa P'$)-{W(CO)$_5$}$_2$] (both Δ_P = 28.5), and [W(CO)$_4$(dppf-κP,P')] (35.6; dppf = 1,1′-bis(diphenylphosphino)ferrocene)[31] and for the pair [W(CO)$_5$(Ph$_2$PfcSMe-κP)] (27.9) and [W(CO)$_4$-(Ph$_2$PfcSMe-$\kappa^2 S$,P)] (36.3).[32,33] In IR spectra of (*E*)-**11** and (*E*)-**12**, the major difference is in the positions of the highest energy ν(C≡O) band (2069 vs 2022 cm^{-1}).

Crystal Structures of 9, (*Z*/*E*)-10, and (*E*)-11. The molecular structure of **9** as determined by single-crystal X-ray diffraction is shown in Figure 5, and the relevant structural parameters are collected in Table 2. The octahedral coordination geometry at tungsten is rather asymmetric as regards the metal−donor distances (W−P and

(27) (a) In an attempt to prepare [W(CO)$_5$(**2**-κP)] we reacted equimolar amounts of [W(CO)$_5$(MeCN)][27b] and **2** in diethyl ether/heptane. However, NMR analysis showed that no reaction took place at room temperature after 24 h. (b) Koelle, U. *J. Organomet. Chem.* **1977**, *133*, 53−58.

(28) Pregosin, P. S.; Kunz, R. W. *^{31}P and C NMR Spectra of Transition Metal Phosphine Complexes* in *NMR Basic Principles and Progress*; Diehl P., Fluck, E., Kosfeld, R., Eds.; Springer: Berlin, 1979; Vol. 16, Section G, pp 99−102 and references therein.

(29) The substitution reactions with [W(CO)$_4$(cod)] at elevated temperature were always accompanied by a partial decomposition resulting into a formation of dark insoluble materials. Decomposing carbonyl complexes are the most likely source of free CO.

(30) The observed changes in the ^{1}H and ^{13}C chemical shifts as compared to uncoordinated (*E*)-**4** can be attributed to electron density changes at the double bond induced by donation from the conjugated phosphorus substituent and an influence of the {W(CO)$_5$} moiety.

(31) Gan, K.-S.; Hor, T. S. A. 1,1′-Bis(diphenylphosphino)ferrocene-Coordination Chemistry, Organic Syntheses, and Catalysis. In *Ferrocenes-Homogeneous Catalysis, Organic Synthesis, Materials Science*; Togni, A., Hayashi, T., Eds.; VCH: Weinheim, Germany, 1995; Chapter 1.2, pp 3−18.

(32) Gibson, V. C.; Long, N. J.; White, A. J. P.; Williams, C. K.; Williams, D. J.; Fontani, M.; Zanello, P. *J. Chem. Soc., Dalton Trans.* **2002**, 3280−3289.

(33) See also the coordination shifts observed for [W(CO)$_5$(L-κP)] complexes featuring 1′-functionalized ferrocene phosphines: Δ_P 28.4 for L = Ph$_2$PfcCHO[20,33a] and 28.5 for L = Ph$_2$PfcCO$_2$H.[33b,c] (a) Meca, L.; Dvořák, D.; Ludvík, J.; Císařová, I.; Štěpnička, P. *Organometallics* **2004**, *23*, 2541−2551. (b) Podlaha, J.; Štěpnička, P.; Císařová, I.; Ludvík, J. *Organometallics* **1996**, *15*, 543−550. (c) Lukešová, L.; Ludvík, J.; Císařová, I.; Štěpnička, P. *Collect. Czech. Chem. Commun.* **2000**, *65*, 1897−1910.

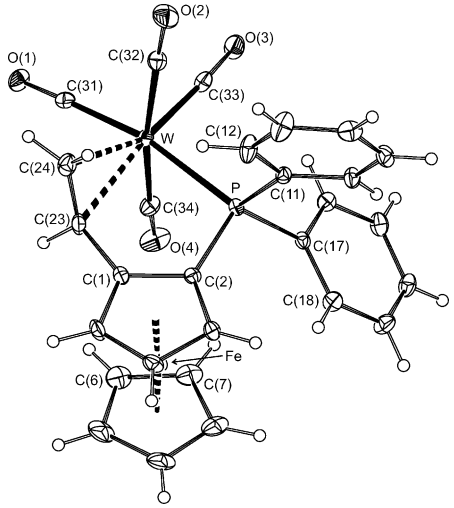

Figure 5. View of the molecular structure of **9**. Displacement ellipsoids enclose 30% probability.

Table 2. Selected Interatomic Distances (Å) and Angles (deg) for **9**[a]

W−P	2.5328(9)	W−C(31)	1.997(4)
W−C(23)	2.455(4)	W−C(32)	2.046(4)
W−C(24)	2.427(4)	W−C(33)	1.976(4)
C(23)−C(24)	1.382(6)	W−C(34)	2.033(4)
C(1)−C(23)	1.488(6)	C(31)−O(1)	1.152(5)
C(2)−P	1.801(4)	C(32)−O(2)	1.129(5)
P−C(11)	1.837(4)	C(33)−O(3)	1.156(5)
P−C(17)	1.835(4)	C(34)−O(4)	1.146(5)
Fe−Cg(1)	1.646(2)	Fe−Cg(2)	1.655(2)
∠Cp(1),Cp(2)	3.2(2)	P−W−Cg(3)	85.6(1)
C(1)−C(23)−C(24)	119.3(4)	P−W−C(23)	79.5(1)
C(2)−C(1)−C(23)	126.6(4)	P−W−C(24)	92.2(1)
C(1)−C(2)−P	117.7(3)	W−C≡O	173.6(4)−177.3(3)
P−W−C(31)	169.0(1)	Cg(3)−W−C(31)	87.0(2)
P−W−C(32)	93.6(1)	Cg(3)−W−C(32)	92.6(2)
P−W−C(33)	98.0(1)	Cg(3)−W−C(33)	174.1(2)
P−W−C(34)	85.3(1)	Cg(3)−W−C(34)	98.8(2)

[a] Definitions are as follows. Ring planes: Cp(1), C(1−5); Cp(2), C(6−10); Cg(1) and Cg(2) are the respective ring centroids. Cg(3) is the midpoint of the η^2-coordinated double bond C(23)═C(24).

W−{η^2-C(23)═C(24)} vs four shorter W−CO bonds); however, the interligand angles do not deviate much from octahedral ones. The highest albeit still rather minor angular deformation is observed for the W−C(34)−O(4) arm (angle at C(34) = 173.6(4)°), which is directed away from the ferrocene unit and toward the phosphine substituent, obviously due to intramolecular steric interactions. In accordance with the better donating ability (and a lower π-acceptor power) of the alkene and phosphine donors as compared with the carbonyls, the W−C(31,33) are slightly shorter than the W−C(32,34) bonds while the respective C−O bond lengths follow the opposite but less pronounced trend. The W−P distance of 2.5328(9) Å corresponds to those in [W(CO)$_5$-(dppf-κP)] (2.563(2) Å),[34] [(OC)$_5$W═C(NEt$_2$)fc**P**Ph$_2$**W**(CO)$_5$] (2.545(1) Å),[33a] and ferrocene chelates [W(CO)$_4$(Ph$_2$PfcSMe-$\kappa^2 S,P$)] (2.538(1) Å)[32] and [W(CO)$_4$(Ph$_2$PfcC(Y)-$\kappa^2 C^1,P$)] (Y = OMe, 2.550(6) Å;[35] Y = NEt$_2$, 2.5391(9) Å[33a]).

Further, the coordination causes lengthening of the double bond (0.06 Å or 4.5% vs **2**). To conform steric demands of the central atom, the double bond is rotated from the Cp1 plane by as much as 64.2(3)° pointing away from the ferrocene unit (cf. the C(2)−C(1)−C(23)−C(24) torsion angle of −78.5(5)°). Similarly to **8**, the P and C(23) atoms are displaced above the Cp1 plane by 0.194(1) and 0.117(4) Å, respectively, and the phosphorus atom is strongly inclined toward the vinyl group (compare C(3)−C(2)−P 134.0(3)° vs C(1)−C(2)−P 117.7(3)°). The W−C(23,24) distances differ by only about 0.03 Å, and the geometry of the whole "W(η^2-C═C)" is similar to those in [W(CO)$_3${(*E*)-(Ph$_2$-PC$_6$H$_4$-2)CH═CHCH$_2$(C$_6$H$_4$PPh$_2$-2)-η^2:$\kappa^2 P,P'$}] (W−C 2.403-(8) and 2.387(9)/C═C 1.36(1) Å)[36] and [W(O)Cl$_2$(PMe$_2$Ph)-{CH$_2$═CHCH$_2$P(O)Ph$_2$)-η^2:κO}] (2.210(6) and 2.228(6)/1.415(8) Å)[37] and W(CO)$_5$ complexes with cyclic alkenes, [W(CO)$_5$(η^2-coe)] (coe = cyclooctene; 2.451(5) and 2.425-(4)/1.384(6) Å)[38] and [W(CO)$_5$(η^2-nbe)] (nbe = norbornene; 2.50(2) and 2.51(2)/1.37(3) Å).[39]

For compound (*Z*/*E*)-**10**, the structural analysis clearly confirmed the tendency of both isomeric forms to cocrystallize. The alkenyl side chain appears statistically disordered, being contributed from *E*- and *Z*-parts in about 1:3 ratio. Furthermore, the structure suffers from a disorder at the phenyl rings which both occupy two positions with nearly equal abundance. As the disorder lowers the overall precision of the structure determination (albeit without making the structural data ambiguous), the structural data will be discussed only briefly here.[40]

The structure of (*Z*/*E*)-**10** is shown in Figure 6 together with the relevant structural data [see also Figure S1 (Supporting Information)]. The coordination polyhedron around tungsten is quite regular: the P−W−CO angles differ by less than 3° from octahedral ones while the OC−W−CO angles reflect bending of the W−C(34)−O(34) arm between

(34) Phang, L.-T.; Au-Yeung, S. C. F.; Hor, T. S. A.; Khoo, S. B.; Zhou, Z.-Y.; Mak, T. C. W. *J. Chem. Soc., Dalton Trans.* **1993**, 165−172.
(35) Butler, I. R.; Cullen, W. R.; Einstein, F. W. B.; Willis, A. C. *Organometallics* **1985**, *4*, 603−604.
(36) Bennett, M. A.; Corlett, S.; Robertson, G. B.; Steffen, W. L. *Aust. J. Chem.* **1980**, *33*, 1261−1273.
(37) Brock, S. L.; Mayer, J. M. *Inorg. Chem.* **1991**, *30*, 2138−2143.
(38) Grevels, F.-W.; Jacke, J.; Klotzbücher, W. E.; Mark, F.; Skibbe, V.; Schaffner, K.; Angermund, K.; Krüger, C.; Lehmann, C. W.; Özkar, S. *Organometallics* **1999**, *18*, 3278−3293.
(39) Górski, M.; Kochel, A.; Szymańska-Buzar, T. *Organometallics* **2004**, *23*, 3037−3046.
(40) Crystallographic data: brown fragment from the reaction batch (0.04 × 0.07 × 0.14 mm^3); tetragonal, space group $P4_12_12$ (No. 92); a = b = 10.7034(4), c = 46.411(2) Å; T = 150(2) K; Z = 8; V = 5317.0-(4) Å^3; D = 1.764 g mL^{-1}; μ(Mo Kα) = 4.962 mm^{-1} (corrected for absorption; transmission factor range, 0.445−0.708). Oxford KM4 CCD diffractometer: 29 441 diffractions ($\theta \le 26.6°$) merged to 5509 unique of which 3987 were regarded as observed ($I > 2\sigma(I)$; R_{int} = 4.17%). Final R-indices: R = 4.44 and wR = 4.92% (all data), R = 2.67% (observed data). Residual electron density: 0.68, −0.50 e Å^{-3}. CCDC: deposition no. 604813. The structure was solved and refined as indicated in Experimental Section with the following restraints: The different alkenyl moieties were refined as two independent contributing parts with the C(23) pivot atom. C(24a,b) and C(25a,b) were refined isotropically, the trans-component having fixed C(23)−C(24b) and C(24b)−C(25b) bond lengths. The refinement resulted in (*E*):(*Z*) occupancies in ca. 1:3 ratio. Phenyl ring carbons were refined over two positions with isotropic displacement parameters and geometry constrained to an ideal hexagon (C−C = 1.39 Å; the refinement converged to nearly 50:50 occupancies for both rings). In addition, several atom pairs from the complementary moieties were included in the model as having identical displacement parameters. All hydrogen atoms were included in calculated positions and refined using the riding model.

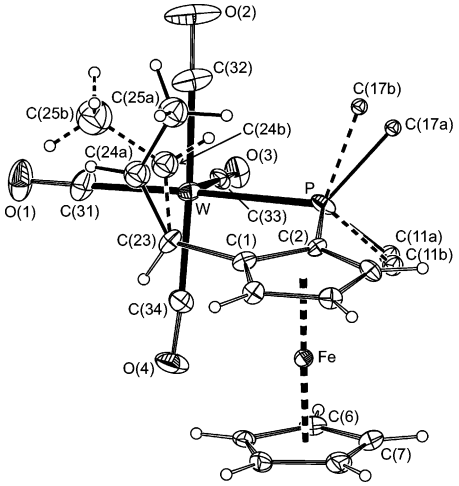

Figure 6. View of the molecular structure of (*Z*/*E*)-**10**. For clarity, the *Z* (solid line, "a") and *E* (dashed line, "b") alkenyl sidearms are shown without bonds to tungsten and only the pivotal atoms from both disordered phenyl rings are included. Displacement ellipsoids are scaled to the 20% probability level. Selected data: W−P 2.520(1), W−C(23) 2.482(4), W−C(24a) 2.560(9), W−C(24b) 2.42(2), W−C(31) 1.963(6), W−C(32) 1.995(6), W−C(33) 1.969(6), W−C(34) 2.007(5), C(23)−C(24a) 1.33(1), C(23)−C(24b) 1.37 (constrained), C(24a)−C(25a) 1.48(1), C(24b)−C(25b) 1.55 (constrained) Å; P−W−C(31) 176.4(2), P−W−C(32) 92.5(2), P−W−C(33) 92.5(2), P−W−C(34) 92.8(1), C(31)−W−C(32) 89.1(3), C(31)−W−C(33) 90.8(2), C(31)−W−C(34) 86.0(2), C(32)−W−C(33) 87.4(2), C(32)−W−C(34) 171.4(2), C(33)−W−C(34) 85.7(2), C(1)−C(23)−C(24a) 125.1(6), C(1)−C(23)−C(24b) 106.5(9), C(23)−C(24a)−C(25a) 120.4(7), C(23)−C(24b)−C(25b) 128(2)°. For alternative drawings, see the Supporting Information.

the C(31) and C(33) atoms, clearly attributable to steric interactions with the ferrocene unit (see above). Unlike **9**, however, complex (*Z*/*E*)-**10** shows very similar W−CO bond lengths. Interestingly, the structure allows for a comparison of the geometry of the W(η^2-C═C) moieties that involve double bonds with the opposite configuration. The moieties seem to differ mainly from steric reasons. Having the ferrocene-bonded carbon C(23) as a common pivot [W−C(23) 2.482(4) Å], the individual double bonds diverge so that the distance from tungsten of the C(24) carbon is larger for the *Z*-configured double bond, where one can expect an increased crowding due to the methyl substitutent [W−C(24a) is 2.560(9) while W−C(24b) is 2.42(2) Å; cf. C(24a)···C(24b) 0.53(2) Å and see Figure S2].

The X-ray diffraction analysis of (*E*)-**11** (Figure 7, Table 3) showed the compound to crystallize with two independent molecules in the asymmetric unit, differing only slightly in mutual orientation of the flexible molecular parts ("$Ph_2PW(CO)_5$"). The coordination polyhedrons around tungsten atoms in both structurally independent molecules are again very regular except that the W−P distances are longer that the bonds to the five carbonyls. Similarly to **9**, the donating ability of the phosphine group is reflected by relative shortening of the W−C(*n*35) bonds ($n = 1$ and 2; trans influence) but has virtually no effect on the C−O bond lengths.

Coordination of the phosphinoalkene as a simple phosphine in (*E*)-**11** is clearly reflected on the overall molecular geometry: the bulky ferrocene "substitutents" ($Ph_2PW(CO)_5$ and (*E*)-CH═CHPh) are rotated away from each other to relieve their possible steric interactions. The W−P bonds are nearly parallel with the Cp1 planes 4.8(2)° [4.3(2)°][41]

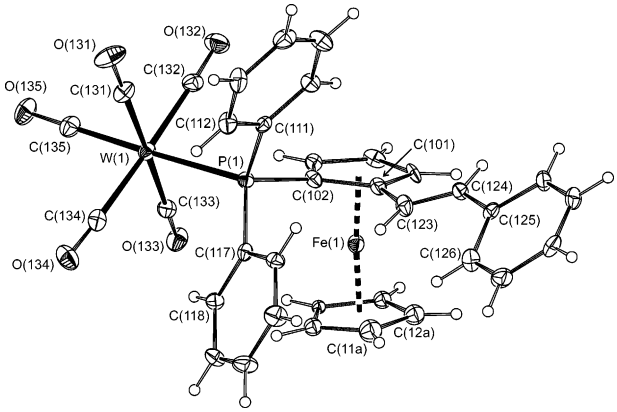

Figure 7. View of molecule 1 in the structure of (*E*)-**11** showing displacement ellipsoids at the 30% probability level. Only one orientation of the disordered cyclopentadienyl ring is shown for clarity. Note: the labeling scheme for molecule 2 is similar with the first digit in the respective atom label changed to two.

while the C(*n*11)−P−C(*n*17) angles appear practically bisected by the same planes. The C(*n*23)−C(*n*24) double bonds show lengths similar to that in (*E*)-stilbene (1.334 Å at 150 K)[42,43] and exhibit no notable torsion attributable to their trans-disposed substituents (the C(*n*01)−C(*n*23)−C(*n*24)−C(*n*25) dihedral angles are −176.2(4)° [−175.6(4)°]). However, the whole β-styryl groups are located above the Cp1 plane and the phenyl and Cp1 rings are far from coplanar. This can be demonstrated by the distances of the C(*n*24) atoms from the Cp1 planes of 0.396(4) Å [0.278(4) Å] and the dihedral angles between the phenyl and Cp1 planes of 44.3(2)° [41.9(2)°].

Electrochemistry. Electrochemical behavior was studied by cyclic voltammetry on a stationary platinum disk and voltammetry on a rotating platinum disk electrode (RDE) in dichloromethane solutions containing the analyte (ca. 5×10^{-4} M) and 0.1 M Bu_4NPF_6 as the supporting electrolyte. The potentials observed for ligands **2** and (*E*)-**4** and their tungsten complexes (**9**, (*E*)-**11**, and (*E*)-**12**) in the anodic region given relative to ferrocene/ferrocenium reference are summarized in Table 4.

Phosphinoalkene **2** undergoes a diffusion-controlled, one-electron reversible oxidation at 0.11 V attributable to the ferrocene/ferrocenium couple (Figure 8d). The position of this wave, indicating a less easy oxidation of **2** than that of ferrocene itself, corresponds with a prevailing electron-accepting nature of the ferrocene substituents ($\sigma_P(PPh_2) = 0.19$, $\sigma_P(CH{=}CH_2) = -0.04$).[44] On going from **2** to chelate complex **9**, the ferrocene/ferrocenium wave shifts by 320 mV anodically, which clearly points to an electron density lowering at the ferrocene unit upon formation of the dative

(41) The numerical values are given as follows: molecule 1 [molecule 2]. Where appropriate, we use generally defined parameters with variable indexes ($n = 1$ for molecule 1, $n = 2$ for molecule 2).

(42) The bond distance was retrieved from the Cambridge Structural Database. For the original reference, see: Harada J.; Ogawa, K. *J. Am. Chem. Soc.* **2001**, *123*, 10884−10888.

(43) Complex [PhC≡W(η^5-C_5HPh_4){(*E*)-($Ph_2PC_6H_4$-2)CH═CHPh-η^2:κP)] where a similar (styryl)phosphine coordinates as an η^2:κP-chelate shows the C═C bond length of 1.450(7) Å: Cairns, G. A.; Carr, N.; Green, M.; Mahon, M. M. *Chem. Commun.* **1996**, 2431−2432.

(44) Hansch, C.; Leo, A.; Taft, R. W. *Chem. Rev.* **1991**, *91*, 165−195.

Table 3. Selected Interatomic Distances (Å) and Angles (deg) for (*E*)-**11**[a]

param	molecule 1 ($n = 1$)	molecule 2 ($n = 2$)	param	molecule 1 ($n = 1$)	molecule 2 ($n = 2$)
W(n)−P(n)	2.562(1)	2.547(1)	P−C(n02)	1.820(4)	1.817(4)
W(n)−C(n31)	2.044(5)	2.048(5)	P−C(n11)	1.832(4)	1.843(4)
C(n31)−O(n31)	1.138(7)	1.151(6)	P−C(n17)	1.835(4)	1.825(4)
W(n)−C(n32)	2.039(4)	2.048(4)	C(n01)−C(n23)	1.464(6)	1.460(6)
C(n32)−O(n32)	1.141(5)	1.138(5)	C(n23)−C(n24)	1.329(6)	1.323(6)
W(n)−C(n33)	2.034(4)	2.044(4)	C(n24)−C(n25)	1.461(6)	1.475(6)
C(n33)−O(n33)	1.147(5)	1.139(5)	C(n01)−C(n23)−C(n24)	123.7(4)	127.3(4)
W(n)−C(n34)	2.054(5)	2.040(4)	C(n23)−C(n24)−C(n25)	127.5(4)	125.1(4)
C(n34)−O(n34)	1.141(6)	1.143(5)	C(n02)−C(n01)−C(n23)	129.3(4)	127.1(4)
W(n)−C(n35)	1.994(5)	1.985(4)	Fe(n)−Cg(n1)	1.638(2)	1.644(2)
C(n35)−O(n35)	1.145(6)	1.161(5)	Fe(n)−Cg(n2)[c]	1.673(3)/1.608(2)	1.663(1)/1.675(1)
P(n)−W(n)−C(n35)[b]	178.1(1)	175.0(1)	∠Cp(n1),Cp(n2)[c]	5.6(3)/6.6(3)	4.0(2)/6.5(2)

[a] Definitions of the ring planes: Cp(n1), C(n01−n05); Cp(n2), C(n06−n10) [Cg(n1) and Cg(n2) are the respective ring centroids]; Ph(n1), C(n25−n30). [b] Other ligand angles: P(1)−W(1)−C(13m) 88.9(1)−94.0(1)°, P(2)−W(2)−C(23m) 90.4(1)−93.2(1)°, $m = 1-4$. Other angles: W(1)−C(13l)−O(13l) 176.0(4)−178.7(3)°, W(2)−C(23l)−O(23l) 175.4(4)−178.0(4)°, $l = 1-5$. [c] Values for two refined positions of the disordered cyclopentadienyl ring are given.

Table 4. Cyclic Voltammteric Data for Ligands **2** and **4** and Their Tungsten−Carbonyl Complexes[a]

compd	$E^{\circ\prime}$(I) (V)	ΔE_p(I) (mV)	$E^{\circ\prime}$(II) (V)	ΔE_p(II) (mV)
2	0.11	80		
4	0.085	90		
9	0.230	80	0.83[b]	
(*E*)-**11**	0.235	70	1.07[b]	
(*E*)-**12**	0.22	80	0.70	80

[a] The potentials are given relative to ferrocene/ferrocenium. $E^{\circ\prime}$ is the formal redox potential determined from cyclic voltammetry performed on dichloromethane solutions containing ca. 5×10^{-4} M analyte and 0.1 M Bu_4NPF_6 at 100 mV/s scan rate. $E^{\circ\prime} = 1/2(E_{pa} + E_{pc})$, where E_{pa} and E_{pc} denote the anodic and cathodic peak potentials, respectively. For all reversible redox processes, the $E^{\circ\prime}$ values were identical with the half-wave potentials ($E_{1/2}$) determined from voltammetry at Pt-RDE (see Experimental Section). Separation of the cyclovoltammetric peak potentials, ΔE_p, is defined as follows: $\Delta E_p = E_{pa} - E_{pc}$. [b] Irreversible vawe. E_{pa} is given.

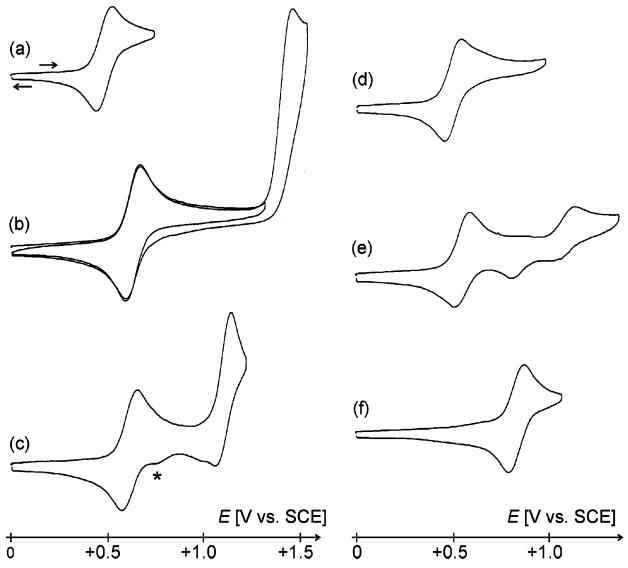

Figure 8. Cyclic voltammograms in anodic region for (*E*)-**4** (a), **10** (b), (*E*)-**11** (c), **2** (d), **6** (e), and **8** (f) as recorded on a platinum disk electrode at the scan rate 100 mV s^{-1}. For conditions, see Table 4. For (*E*)-**11**, an asterisk indicates a minor return peak attributable to adsorption or decomposition products.

bonds. The magnitude of the coordination shift is strikingly higher than that observed for *P*-monodentate ferrocene ligands: [W(CO)$_5$(L-κP)], where L = $FcPPh_2$ (190 mV)[45] and Ph_2PfcCO_2H (180 mV),[33c] which can be ascribed to coordination of **2** as a bidentate chelating donor.

The presence of the W(CO)$_4$ moiety in **9** is further reflected by an additional wave at 0.83 V (E_{pa}) due to a tungsten-centered oxidation. The height of the wave is about double that of the first oxidation, indicating a two-electron process.[46] The oxidation is irreversible at all scan rates employed (up to 500 mV s^{-1}). However, it remains diffusion controlled as established by linear dependence of the anodic peak current (i_{pa}) on the square root of the scan rate (υ; $i_{pa} \propto \upsilon^{1/2}$)[47] and, above all, does not affect the preceding ferrocene/ferrocenium oxidation. Such a redox response parallels the behavior of [W(CO)$_6$], which is oxidized at platinum electrode in a diffusion-controlled, irreversible bielectronic process (ECE mechanism) at around 1.13 V (in MeCN solution).[48] Complexes [W(CO)$_5$(L-κP)] mentioned above undergo similar oxidation at higher potentials: L = $FcPPh_2$ (0.97 V; Fc = ferrocenyl) and Ph_2PfcCO_2H (0.98 V), which again corresponds with a replacement of two carbonyls with less π-accepting "donors" in **9**.[49]

The series involving ligand (*E*)-**4** is more complete (Figure 8a−c). Similarly to **2**, compound (*E*)-**4** undergoes reversible ferrocene-centered oxidation. In accordance with the overall substituent effect (σ_p(CH=CHPh) = −0.07),[44] the observed redox potential is very slightly lower than for **2**. Oxidation pattern observed for the pentacarbonyl complex (*E*)-**11** is analogous to the behavior of its [W(CO)$_5$(L-κP)] counterparts (see above) in that it undergoes a reversible oxidation at the ferrocene unit followed by irreversible multielectron, tungsten-centered oxidation at ca. 1.07 V. Finally, compound (*E*)-**12** follows the oxidation sequence observed for **9** (though at lower potentials) with only exception in that the second oxidation shows clear signs of electrochemical quasi-

(45) Kotz, J. C.; Nivert, C. L., Lieber, J. M.; Reed, R. C. *J. Organomet. Chem.* **1975**, *91*, 87−95.
(46) The same applies to voltammetric waves observed at Pt-RDE.
(47) The anodic peak current (E_{pa}) shifts slightly to higher potentials upon raising the scan rate.
(48) (a) Pickett, C. J.; Pletcher, D. *J. Chem. Soc., Dalton Trans.* **1975**, 879−886. The E_p value was recalculated from the original reference (E_p = +1.53 V vs SCE in MeCN containing 0.2 M Bu_4NBF_4) taking $E^{\circ\prime}$(ferrocene/ferrocenium) = 0.40 V as obtained in acetonitrile with 0.1 M Bu_4NPF_6. For a reference, see: (b) Connelly, N. G.; Geiger, E. *Chem. Rev.* **1996**, *96*, 877−910.
(49) Under similar conditions, complex [W(CO)$_5$(dppf-κP)] shows two successive oxidation at 0.34 V (ferrocene/ferrocenium, reversible) and 1.00 V (W-centered, irreversible) but with *similar* peak currents: Ohs, A. C.; Rheingold, A. L.; Shaw, M. J.; Nataro, C. *Organometallics* **2004**, *23*, 4655−4660.

reversibility: while the oxidation appears fully irreversible at 20 mV/s (the ratio of the peak currents, $i_{pc}/i_{pa} = 0$), an increase of the scan rate results in an increase of the i_{pc}/i_{pa} ratio up to values close to unity at 500 mV/s. Such behavior is very likely invoked by chemical complications associated with the electrochemical oxidation that (relatively slowly) consume the electrogenerated species. Remarkably, the irreversibility of the metal-centered oxidation in (*E*)-**11** or (*E*)-**12** does not influence the redox response of the ferrocene/ferrocenium couple.

The redox behavior of palladium complexes **6** and **8** is markedly different from the tungsten complexes. Compound **8** shows only single oxidation within the experimentally accessible region ($E^{\circ\prime} = 0.43$ V; Figure 8f). The wave can be ascribed one-electron, reversible oxidation at the ferrocene moiety and occurs shifted by 320 mV anodically as compared with uncoordinated **2** (Figure 8d).[50] As shown in Figure 8e, the anodic pattern observed for **6** is more complicated. In the anodic region, the complex first undergoes a diffusion-controlled reversible, one-electron oxidation at 0.155 V, clearly attributable to ferrocene-centered oxidation. In accordance with **6** being a neutral complex that possesses an additional (chloride) ligand, the wave is shifted by only +45 mV vs **2**. At higher potentials, the monooxidized species undergoes two successive, well-separated oxidations at 0.43 V ($\Delta E_p = 60$ mV) and 0.69 V (ΔE_p ca. 80 mV).[51] Since the second oxidation is found at exactly the same position as the only wave observed for **8**, one can assume some chemical reactions following the prior ferrocene oxidation to generate another electroactive species, possibly similar to **8**.

Concluding Remarks

Ferrocene-based, planar-chiral alkenylphosphines **2**−**4** are accessible conveniently and in very good yields by olefination of the chiral phosphinoaldehyde **1**. Depending on the alkenylation procedure, the compounds can be obtained as double bond configurational isomers; however, methods leading to isomer mixtures should be avoided due to difficulties with isomer separation. The alkenylphosphines represent the first organometallic analogues[52] to the known organic alkenyl-substituted triphenylphosphines.[13] As demonstrated for the series of palladium(II) and tungsten(0)−carbonyl complexes, the ferrocene alkenylphosphines coordinate as *P*-monodentate or η^2:κP-chelating donors, similarly to their organic counterparts. A conversion of monodentate **2** into its chelate form was established for the pair of palladium(II) complexes **6** and **8**. The structural data collected indicate that coordination in either mode is facilitated by flexibility of the donor groups attached to the rigid ferrocene scaffold. Further studies on the reactivity of ferrocene alkenylphosphines are currently under way.

Experimental Section

General Comments. Unless noted otherwise, the syntheses were performed under an argon atmosphere and with an exclusion of the direct daylight. Tetrahydrofuran (THF) was distilled from potassium−benzophenone ketyl. Toluene, diethyl ether, and hexane were dried over sodium or potassium metals and distilled. Dichloromethane was predried with anhydrous potassium carbonate and then distilled from calcium hydride. Compounds **1**,[16] **5**,[53] and **7**[22] were synthesized by the literature procedures. Other chemicals and solvents were used as received from commercial sources (Fluka, Aldrich; solvents from Lach-Ner). The reported yields are not optimized.

NMR spectra were measured on a Varian UNITY Inova 400 spectrometer (^{1}H, 399.95; ^{13}C, 100.58; ^{31}P, 161.90 MHz) at 298 K. Chemical shifts (δ/ppm) are given relative to internal tetramethylsilane (^{1}H and ^{13}C) or an external 85% aqueous H_3PO_4 (^{31}P). IR spectra were recorded on an FT IR Nicolet Magna 760 instrument in the range of 400−4000 cm^{-1}. Mass spectra were obtained on a Varian 3400/Finnigan MAT INCOS (GC-EI MS) or ZAB-SEQ VG Analytical (direct inlet EI, FAB and HR MS analyses) spectrometers. Electrospray (ESI) mass spectra were recorded for methanol solutions on a Bruker Esquire 3000 spectrometer. CD spectra were obtained on a JASCO J-810 spectrometer (methanol solutions: $c = 1.34$ mM for **2**, 0.78 mM for **6**, and 0.75 mM for **8**) while UV−vis spectra were recorded in the same solvent on a Unicam UV 300 spectrometer ($c = 1.0$ mM, $l = 1$, and 10 mm). Melting points were determined on a Kofler apparatus and are uncorrected.

Electrochemical measurements were performed on a multipurpose polarograph PA3 interfaced to a model 4103 XY recorded (Laboratorní přístroje, Prague) at room temperature using a standard three-electrode cell: rotating or stationary platinum disk working electrode (1 mm diameter), platinum sheet auxiliary electrode, and saturated calomel electrode (SCE) reference electrode, separated from the analyzed solution by a salt bridge filled with 0.1 M Bu_4NPF_6 in dichloromethane. The samples were dissolved in dichloromethane (Merck, p.a.) to give ca. 5×10^{-4} M concentration of the analyte and 0.1 M Bu_4NPF_6 (supporting electrolyte; Fluka, purissimum for electrochemistry). The samples were deaerated with argon prior to the measurement and then kept under an argon blanket. Cyclic voltammograms were recorded at stationary platinum disk electrode (scan rates 20−500 mV/s), while the voltammograms were obtained at rotating disk electrode (500 rpm, scan rates 10−100 mV/s). Note: the redox potentials in Table 4 and text are given relative to ferrocene/ferrocenium reference whereas Figure 8 shows the curves "as recorded", i.e., with SCE as the reference.

(50) The potential shift is similar to that observed for the pair dppf/[$PdCl_2$(dppf)] as determined in 1,2-$C_2H_4Cl_2$ ($E_{pa} = 0.64$ V/$E^{\circ\prime} = 1.03$ V vs SCE)[50a] and MeCN solutions ($E_{pa} = 0.51$ V/$E^{\circ\prime} = 0.88$ V vs SCE).[50b] (a) Corain, B.; Longato, B.; Favero, G.; Ajó, D.; Pilloni, G.; Russo, U.; Kreissl, F. R. *Inorg. Chim. Acta* **1989**, *18*, 583−590. (b) Housecroft, C. E.; Owen, S. M.; Raithby, P. R.; Shayjk, B. A. M. *Organometallics* **1990**, *9*, 1617−1623.

(51) The observed pattern does not change significantly with the scan rate (20−500 mV/s) or upon repeated cycling. When the sample is scanned with switching potential set before the second oxidation, the first wave is observed with full reversibility ($i_{pa} \propto \nu^{1/2}$, $i_{pa}/i_{pc} \approx 1$). Cycling in the whole accessible anodic region (i.e. with the switching pontential set after the third oxidation wave) lowers the reversibility of the first wave as indicated by $i_{pa} > i_{pc}$. In the voltammogram recorded at RDE, the wave due to the ferrocene oxidation exerts the normal sigmoidal shape and a height corresponding to one electron exchanged while the third oxidation is observed as a tilted irreversible wave of approximately half-height of the first wave. The second wave from cyclic voltammogram is *not* reflected at all in the voltammogram at RDE.

(52) It is noteworthy that planar-chiral arene−tricarabonylchromium(0) complexes, [$Cr(CO)_3$(η^6-C_6H_4(X-1)(PPh_2-2))], where X = CH═CH_2 and CH_2CH═CH_2, were reported. However, no coordination study was made. Christian, P. W. N.; Gil, R.; Muñiz-Fernández, K.; Thomas, S. E.; Wierzchleyski, A. T. *J. Chem. Soc., Chem. Commun.* **1994**, 1569−1570.

(53) Cope, A. C.; Friedrich, E. C. *J. Am. Chem. Soc.* **1968**, *90*, 909−913.

Preparation of (S_p)-2-(Diphenylphosphino)-1-vinylferrocene (2). Butyllithium (2.2 mL, 2.5 M in hexanes, 5.5 mmol) was slowly introduced to a stirred suspension of [PPh_3Me]Br (2.146 g, 6.0 mmol) in THF (50 mL) with cooling in an ice bath. The white phosphonium salt dissolved almost completely to give an orange solution, which later turned to bright yellow. After stirring of the solution at 0 °C for 30 min, a solution of (S_p)-2-(diphenylphosphino)ferrocenecarboxaldehyde (**1**; 1.995 g, 5.0 mmol) in THF (25 mL) was added to the formed ylide and the cooling bath was removed. The reaction mixture was stirred for another 6 h at room temperature and then quenched by addition of saturated aqueous $NaHCO_3$ and stirring for another 15 min. The orange organic phase was separated, washed successively with saturated aqueous $NaHCO_3$ and NaCl solutions, dried over $MgSO_4$, and evaporated under reduced pressure. The oily residue was purified by column chromatography (silica gel, 1:2 hexane−diethyl ether). The major band of the product is eluted first, followed by a minor band of the respective phosphine oxide. Evaporation of the first fraction under vacuum (finally at 0.1 Torr for 1 h) gave the phosphinoalkene as an amber oil, which was immediately dissolved in hot heptane. Subsequent crystallization of the solution at room temperature and then at −18 °C gave analytically pure **2** as a rusty brown crystalline solid, which was isolated by suction. Yield: 1.750 g (88%).

Mp: 140−141 °C (heptane). ^{1}H NMR ($CDCl_3$): δ 3.71 (dt, 1 H, C_5H_3), 4.02 (s, 5 H, C_5H_5), 4.33 (dt, 1 H, C_5H_3), 4.73 (dt, 1 H, C_5H_3), 5.03 (dd, $^3J_{HH}$ = 10.8, $^2J_{HH}$ = 1.5 Hz, 1 H, =CH_2), 5.38 (dt, $^3J_{HH}$ = 17.5, $^2J_{HH} \approx J_{PH} \approx$ 1.5 Hz, 1 H, =CH_2), 6.07 (ddd, $^3J_{HH}$ = 10.8, 17.5, J_{PH} = 2.2 Hz, 1 H, =CH), 7.11−7.59 (m, 10 H, PPh_2). ^{13}C{^{1}H} NMR ($CDCl_3$): δ 67.71 (d, J_{PC} = 3 Hz, CH of C_5H_3), 70.02 (CH of C_5H_3), 70.34 (C_5H_5), 71.98 (d, J_{PC} = 4 Hz, CH of C_5H_3), 75.56 (d, $^1J_{PC}$ = 9 Hz, *C*P of C_5H_3), 88.79 (d, $^2J_{PC}$ = 21 Hz, *C*CH=CH_2 of C_5H_3), 112.36 (d, $J_{PC} \approx$ 2 Hz, =CH_2), 127.72, 128.06 (d, J_{PC} = 6 Hz), 128.12 (d, J_{PC} = 8 Hz), 129.14, 132.00 (d, J_{PC} = 18 Hz) (CH of PPh_2); 132.24 (d, J_{PC} = 12 Hz, =CH), 135.16 (d, J_{PC} = 21 Hz, CH of PPh_2), 137.13 (d, $^1J_{PC}$ = 9 Hz), 139.72 (d, $^1J_{PC}$ = 9 Hz) (2 × C_{ipso} of PPh_2). ^{31}P{^{1}H} NMR ($CDCl_3$): δ −21.3 (s). IR (Nujol): ν/cm^{-1} 1631 (w), 1614 (m), 1585 (w) ν(C=C); 1310 (m), 1246 (m), 1167 (s), 1105 (m), 1037 (m), 1002 (m), 988 (m), 900 (s), 827 (s), 811 (s), 745 (vs), 697 (vs), 624 (m), 573 (m), 508 (m), 476 (s), 454 (s). EI MS [*m*/*z* (relative abundance)]: 397 (27), 396 ($M^{+\bullet}$, 100), 395 (18), 394 (7), 331 (22, [M − C_5H_5]$^+$), 329 (10), 319 ([M − Ph]$^+$, 7), 288 (19), 275 (12), 252 (16), 226 (5), 198 (6), 197 (9), 196 (14), 183 (11), 176 (17), 171 (6), 170 (7), 165 (19), 152 (10), 151 (6), 133 (8), 121 ([C_5H_5Fe]$^+$, 28), 120 (7), 56 (Fe, 28). [α]$_D$ = +343 (*c* = 0.50, $CHCl_3$). Anal. Calcd for $C_{24}H_{21}FeP$: C, 72.75; H, 5.34. Found: C, 72.50; H, 5.37.

Preparation of (S_p)-2-(Diphenylphosphino)-1-(prop-1-en-1-yl)ferrocenes ((*Z*/*E*)-3). Butyllithium (0.6 mL 2.5 M in hexanes, 1.5 mmol) was added dropwise to a suspension of [PPh_3Et]Br (0.559 g, 1.5 mmol) in dry THF (30 mL) at 0 °C. Nearly all the white phosphonium salt dissolved to give an orange solution, which was stirred 0 °C for another 15 min and then treated with a solution of **1** (398 mg, 1.0 mmol) in THF (20 mL). The mixture was stirred for 30 min at 0 °C and overnight at 60 °C (temperature in bath). Then, it was quenched by addition of saturated aqueous NaCl solution and diluted with diethyl ether. The organic layer was separated, washed with brine, dried ($MgSO_4$), and evaporated under vacuum. The orange brown oily residue was purified by column chromatography on silica gel using hexane−diethyl ether (10:1) as the eluent. The first orange band was collected and evaporated. The residue was dissolved in warm heptane (8 mL) and the solution filtered and crystallized at −18 °C to give rusty brown crystalline solid, which was isolated by decantation and dried under vacuum. Yield: 235 mg (57%). The product was shown NMR spectroscopically to be a mixture of double bond isomers, (*Z*)-**3** and (*E*)-**3**, in ca. 5:1 ratio. Attempts to fully separate the double-bond isomers by either chromatography or crystallization failed.

HR MS (EI): calcd for $C_{25}H_{23}{}^{56}FeP$, 410.0887; found 410.0899. Major isomer, (*Z*)-**3**: ^{1}H NMR ($CDCl_3$) δ 1.79 (dd, $^3J_{HH}$ = 7.1, $^4J_{HH}$ = 1.7 Hz, 3 H, Me), 3.67 (m, 1 H, C_5H_3), 4.03 (s, 5 H, C_5H_5), 4.33 (apparent t, 1 H, C_5H_3), 4.70 (m, 1 H, C_5H_3), 5.58 (dq, $^3J_{HH}$ = 11.4, 7.1 Hz, 1 H, =C*H*Me), 6.43 (ddq, $^3J_{HH}$ = 11.4, $^4J_{HH} \approx {}^4J_{PH} \approx$ 1.7 Hz, 1 H, C*H*=CHMe), 7.07−7.59 (m, 10 H, PPh_2); ^{31}P{^{1}H} NMR ($CDCl_3$) δ −20.8. Minor isomer, (*E*)-**3**: ^{1}H NMR ($CDCl_3$) δ 1.69 (dd, $^3J_{HH}$ = 6.6, $^4J_{HH}$ = 1.7 Hz, 3 H, Me), 3.68 (m, 1 H, C_5H_3), 4.00 (s, 5 H, C_5H_5), 4.28 (apparent t, 1 H, C_5H_3), 4.66 (m, 1 H, C_5H_3), 5.86 (ddq, $^3J_{HH}$ = 15.6, $^5J_{PH}$ = 1.1, $^3J_{HH}$ = 6.6 Hz, 1 H, =C*H*Me), 6.39 (ddq, $^3J_{HH}$ = 15.6, $^4J_{HH} \approx {}^4J_{PH} \approx$ 1.7 Hz, 1 H, C*H*=CHMe), 7.07−7.59 (m, 10 H, PPh_2); ^{31}P{^{1}H} NMR ($CDCl_3$): δ −21.2.

Preparation of (*E*,S_p)-2-(Diphenylphosphino)-1-(2-phenylethen-1-yl)ferrocene ((*E*)-4). Butyllithium (0.8 mL 2.5 M in hexanes, 2.0 mmol) was added to a solution of $PhCH_2P(O)(OEt)_2$ (0.65 mL, 3.1 mmol) in THF (25 mL) with cooling to −78 °C and the resulting mixture stirred for 30 min. A solution of **1** (402 mg. 1.0 mmol) in THF (25 mL) was introduced, the cooling bath was removed, and the mixture stirred for 90 min at room temperature and, finally, slowly brought to 60 °C and stirred at this temperature overnight. The reaction was terminated by addition of saturated aqueous NaCl solution and the mixture diluted with diethyl ether. The organic layer was separated, washed with brine, dried ($MgSO_4$), and evaporated under vacuum. The brown residue was purified by column chromatography on silica gel with hexane−diethyl ether (4:1). The first orange band was collected and evaporated. The solid residue was dissolved in hot heptane (15 mL) and the solution filtered while warm and crystallized at −18 °C to give a brown crystalline solid. The separated product was filtered off, washed with a little pentane, and dried under vacuum. Yield of (*E*)-**4**: 286 mg (61%), rusty brown crystalline solid.

^{1}H NMR ($CDCl_3$): δ 3.84 (m, 1 H, C_5H_3), 4.06 (s, 5 H, C_5H_5), 4.43 (apparent t, 1 H, C_5H_3), 4.88 (m, 1 H, C_5H_3), 6.77 (dd, $^3J_{HH}$ = 16.2, $J_{PC} \approx$ 1 Hz, CH=), 7.13−7.64 (m, 16 H, Ph, PPh_2 and CH=). ^{13}C{^{1}H} NMR ($CDCl_3$): δ 67.45 (d, J_{PC} = 4 H, CH of C_5H_3), 70.33 (C_5H_5), 70.46 (s, CH of C_5H_3), 72.37 (d, J_{PC} = 4 H, CH of C_5H_3), 76.12 (d, $^1J_{PC}$ = 9 H, CP of C_5H_3), 88.71 (d, $^2J_{PC}$ = 21 H, *C*CH=CH of C_5H_3), 125.40 (d, $^3J_{PC}$ = 12 Hz, *C*H=CHPh), 125.98 (CH of Ph), 126.85 (CH of Ph or PPh_2), 126.97 (d, $^4J_{PC}$ = 2 Hz, CH=*C*HPh), 127.75 (CH of Ph or PPh_2), 128.11 (d, J_{PC} = 6 Hz), 128.18 (d, J_{PC} = 7 Hz) (2 × CH of Ph); 128.54 (CH of Ph), 129.22 (CH of Ph or PPh_2), 132.02 (d, J_{PC} = 18 Hz), 135.21 (d, J_{PC} = 21 Hz) (2 × CH of PPh_2); 137.17 (d, $^1J_{PC}$ = 9 Hz, C_{ipso} of PPh_2), 137.72 (C_{ipso} of Ph), 139.74 (d, $^1J_{PC}$ = 10 Hz, C_{ipso} of PPh_2). ^{31}P{^{1}H} NMR ($CDCl_3$): δ −21.7 (s). IR (Nujol) (ν/cm^{-1}): 1633 (m), 1598 (w), 1584 (m); 1250 (m), 1202 (m), 1164 (s), 1107 (m), 1096 (m), 1070 (m), 1039 (m), 1003 (m), 956 (s), 819 9s), 740 (vs), 694 (vs), 588 (m), 526 (m), 511 (s), 487 (s), 479 (s), 462 (s), 444 (m), 430 (m). MS (EI) [*m*/*z* (relative abundance)]: 474 (16), 473 (34), 472 ($M^{+\bullet}$), 407 (6), 405 (5), 165 (6), 121 (7, [C_5H_5Fe]$^+$). HR MS (EI): calcd for $C_{30}H_{25}{}^{56}FeP$, 472.1043; found 472.1051. Anal. Calcd for $C_{30}H_{25}FeP$: C, 76.28; H, 5.34. Found: C, 76.17; H, 5.18.

Preparation of [*SP*-4-4]-Chloro[2-{(dimethylamino-κN)methyl}phenyl-κC^1][(S_p)-2-(diphenylphosphino-κP)-1-vinylferrocene]-palladium(II) (6). Bis(μ-chloro)bis{[2-(dimethylamino-κN)phenyl-κC^1]palladium(II)} (**5**; 56 mg, 0.1 mmol) and **2** (80 mg, 0.2 mmol),

were dissolved in dichloromethane (2 mL). The clear orange reaction solution was stirred for 1 h at room temperature and then evaporated under vacuum to give an orange foam, which was extracted with heptane (25 mL). The extract was filtered while hot, allowed to cool to room temperature, and then stored at −18 °C overnight. The separated material was filtered off, washed with pentane, and dried under vacuum. Yield of **6**: 84 mg (62%), orange powdery solid. Note: the crude product obtained by evaporation of the reaction mixture is essentially pure but typically contains traces of the solvent.

^{1}H NMR ($CDCl_3$): δ 2.80 (d, $^4J_{PH}$ = 2.5 Hz, 3 H, NMe_2), 2.84 (d, $^4J_{PH}$ = 2.6 Hz, 3 H, NMe_2), 3.94 (dd, $^2J_{HH}$ = 13.3, $^4J_{PH}$ = 2.7 Hz, 1 H, NCH_2), 4.14 (dd, $^2J_{HH}$ = 13.3, $^4J_{PH}$ = 2.1 Hz, 1 H, NCH_2), 4.20 (s, 5 H, C_5H_5), 4.51 (br apparent t, 1 H, C_5H_3), 4.79 (dt, J = 2.6, ca. 1.2 Hz, 1 H, C_5H_3), 4.82 (m, 1 H, C_5H_3), 4.89 (dd, $^3J_{HH}$ = 10.8, $^2J_{HH}$ = 1.7 Hz, 1 H, =CH_2), 5.35 (dd, $^3J_{HH}$ = 17.3, $^2J_{HH}$ = 1.7 Hz, 1 H, =CH_2), 6.30−6.39 (m, 2 H, C_6H_4), 6.60 (dd, $^3J_{HH}$ = 17.3, 10.8 Hz, 1 H, CH=), 6.75−6.96 (m, 2 H, C_6H_4), 7.27−7.85 (m, 10 H, PPh_2). ^{13}C{^{1}H) NMR ($CDCl_3$): δ 50.03, 50.64 (2 × d, $^3J_{PC}$ = 2 Hz, NMe_2); 69.22 (d, J_{PC} = 6 Hz, CH of C_5H_3), 70.19 (d, J_{PC} = 9 Hz, CH of C_5H_3), 71.40 (C_5H_5), 72.41 (d, $^1J_{PC}$ = 49 Hz, C−P of C_5H_3), 73.42 (d, $^3J_{PC}$ = 3 Hz, NCH_2), 78.35 (d, J_{PC} = 15 Hz, CH of C_5H_3), 87.76 (d, $^2J_{PC}$ = 8 Hz, C−CH=CH_2 of C_5H_3), 113.18 (=CH_2), 121.99, 123.45 (2 × CH of C_6H_4); 124.70 (d, J_{PC} = 6 Hz, CH of C_6H_4), 127.50 (d, J_{PC} = 11 Hz, CH of PPh_2), 127.56 (d, J_{PC} = 13 Hz, CH of PPh_2), 129.96, 130.27 (2 × d, J_{PC} = 11 Hz, CH of PPh_2); 132.36, 133.72 (2 × d, $^1J_{PC}$ = 52 Hz, C_{ipso} of PPh_2); 134.15 (=CH), 134.49, 135.21 (2 × d, J_{PC} = 12 Hz, CH of PPh_2); 137.97 (d, J_{PC} = 11 Hz, CH of C_6H_4), 147.69 (d, J_{PC} = 2 Hz, C_{ipso} of C_6H_4), 152.58 (d, J_{PC} = 1 Hz, C_{ipso} of C_6H_4). ^{31}P{^{1}H) NMR ($CDCl_3$): δ +31.4 (s). IR (Nujol) (ν/cm^{-1}): ν(C=C) 1668 (s); 1579 (w), 1297 (m), 1160 (m), 1098 (m), 1026 (w), 999 (w), 972 (w), 934 (w), 844 (m), 827 (m), 742 (s), 695 (s), 519 (m), 496 (m), 489 (m), 471 (m). ESI+ MS: m/z 636 ([$C_{33}H_{33}{}^{56}Fe^{14}N^{31}P^{106}$-Pd]$^+$ ≡ [M − Cl]$^+$; experimental isotopic pattern fits the theoretical one). Anal. Calcd for $C_{33}H_{33}ClFeNPPd$: C, 58.95; H, 4.95; N, 2.08. Found: C, 58.76; H, 4.93; N, 1.79.

Preparation of [*SP*-4-2]-[2-{(Dimethylamino-κN)methyl}-phenyl-κC^1][(S_p)-2-(diphenylphosphino-κP)-1-(η^2-vinyl)ferrocene]-palladium(II) Perchlorate (8). Bis(acetonitrile)[2-(dimethylamino-κN)phenyl-κC^1]palladium(II) perchlorate (**7**; 85 mg, 0.20 mmol) and **2** (80 mg, 0.2 mmol) were dissolved in chloroform (3 mL). After being stirring in the dark for 3 h, the reaction solution was filtered and slowly precipitated with hexane. The mixture was allowed to stand at 0 °C for 3 h, and the separated solid was filtered off, washed with diethyl ether, and dried under vacuum. The yield of **8** is essentially quantitative; however, the product retains the solvents. An analytical sample of **8** in the form of dark red brown crystals was obtained by recrystallization from dichoromethane−diethyl ether.

^{1}H NMR ($CDCl_3$): δ 2.70 (d, $^4J_{PH}$ = 2.2 Hz, 3 H, NMe_2), 3.13 (d, $^4J_{PH}$ = 3.7 Hz, 3 H, NMe_2), 3.79 (dd, $^2J_{HH}$ = 13.7, $^4J_{PH}$ = 3.9 Hz, 1 H, NCH_2), 3.98 (apparent qi, $J \approx$ 1.4 Hz, 1 H, C_5H_3), 4.31 (s, 5 H, C_5H_5), 4.71 (td, J = 2.6, 0.6 Hz, 1 H, C_5H_3), 4.74 (br d, $^2J_{HH} \approx$ 13.4 Hz, 1 H, NCH_2), 5.12 (br d, $^3J_{HH}$ = 16.5 Hz, 1 H, =CH_2), 5.12 (dt, J = 2.4, 1.2 Hz, 1 H, C_5H_3), 5.28 (br dd, $^3J_{HH}$ = 9.6, $J \approx$ 1.3 Hz, 1 H, =CH_2), 6.73−7.23 (m, 4 H, C_6H_4), 7.33 (dd, $^3J_{HH}$ = 16.5, 9.6 Hz, 1 H, CH=), 7.40−7.69 (m, 10 H, PPh_2). ^{13}C-{^{1}H} NMR ($CDCl_3$): δ 49.91 (d, $^3J_{PC}$ = 2 Hz, NMe_2), 52.58 (d, $^3J_{PC} \approx$ 2 Hz, NMe_2), 71.05 (CH of C_5H_3; δ_H 3.98), 71.80 (C_5H_5), 73.00 (d, J_{PC} = 3 Hz, CH of C_5H_3; δ_H 5.12), ca. 73.0 (br, NCH_2), 75.58 (d, J_{PC} = 7 Hz, CH of C_5H_3; δ_H 4.71), 90.25 (d, $^2J_{PC}$ = 21 Hz, C-CH=CH_2 of C_5H_3), 100.93 (=CH_2), 124.11 (CH of C_6H_4), 125.28 (d, $^1J_{PC}$ = 59 Hz, C_{ipso} of PPh_2), 126.69 (d, J_{PC} = 7 Hz, CH of C_6H_4), 126.90 (CH of C_6H_4), 128.49 (d, J_{PC} = 11 Hz, CH of PPh_2), 129.62 (d, J_{PC} = 11 Hz, CH of PPh_2), 131.38 (d, $^1J_{PC}$ = 49 Hz, C_{ipso} of PPh_2), 131.88 (d, J_{PC} = 2 Hz, CH of PPh_2), 132.21 (d, J_{PC} = 12 Hz, CH of PPh_2), 132.42 (d, J_{PC} = 2 Hz, CH of PPh_2), 133.21 (=CH), 135.33 (d, J_{PC} = 12 Hz, CH of PPh_2), 138.88 (d, J_{PC} = 12 Hz, CH of C_6H_4), 148.14 (d, J_{PC} = 2 Hz, C_{ipso} of C_6H_4), 151.53 (d, $J_{PC} \approx$ 1 Hz, C_{ipso} of C_6H_4); the signal due to C-PPh_2 at C_5H_3 was not found. ^{31}P{^{1}H} NMR ($CDCl_3$): δ +30.0 (s). IR (Nujol) (ν/cm^{-1}) 1579 (w), 1570 (m), 1229 (m), 1172 (w), $\nu_3(ClO_4)$ 1107−1084 (vs, composite); 1000 (m), 940 (m), 844 (s), 746 (s), 698 (m), $\nu_4(ClO_4)$ 623 (s); 560 (w), 527 (m), 517 (m), 496 (m), 472 (m), 455 (m). ESI+ MS: m/z 636 ([$C_{33}H_{33}{}^{56}Fe^{14}N^{31}P^{106}Pd$]$^+$, the cation; experimental and calculated isotopic patterns agree). Anal. Calcd for $C_{33}H_{33}ClFeNO_4PPd$: C, 53.83; H, 4.52; N, 1.90. Found: C, 53.58; H, 4.58; N, 1.83.

Conversion of 6 to 8. An NMR Study. A solution of silver(I) perchlorate (6.3 mg, 30 mol) in dry acetonitrile (0.5 mL) was added to a dichloromethane solution of **6** (17.0 mg, 25 μmol in 1 mL), causing immediate separation of an off-white precipitate (AgCl). The mixture was stirred in the dark for 30 min, filtered, and evaporated. The residue was extracted with dichloromethane (ca. 3 mL), the extract diluted with hexane (ca. 1 mL), and the mixture filtered to remove silver salts. After evaporation of the filtrate, the residue was dissolved in $CDCl_3$ and analyzed by ^{1}H, ^{13}C, and ^{31}P NMR spectroscopy. The spectra clearly showed an exclusive formation of **8**.

Preparation of Tetracarbonyl[(S_p)-2-(diphenylphosphino-κP)-1-(η^2-vinyl)ferrocene]tungsten(0) (9). Toluene (8 mL) was added to solid [W(cod)(CO)$_4$] (81 mg, 0.20 mmol) and **2** (80 mg, 0.20 mmol), and the mixture was heated at gentle reflux for 3 h. The solid educts quickly dissolved to give a clear orange solution. Then, the reaction solution was cooled to room temperature and filtered through a short silica gel column (elution with toluene) to remove decomposition products. The orange eluate was evaporated under reduced pressure to give an oily residue, which was immediately extracted with hot heptane. The extract was filtered while hot and allowed to crystallize at room temperature and then at 0 °C overnight to yield **9** as orange needles, which were isolated by suction and dried under vacuum. Yield: 126 mg (91%).

^{1}H NMR ($CDCl_3$): δ 3.21 (ddd, $^3J_{HH}$ = 13.4, J_{PH} = 2.1, $^2J_{HH} \approx$ 0.5 Hz, 1 H, =CH_2), 3.72 (ddd, $^3J_{HH}$ = 9.0, J_{PH} = 3.3, $^2J_{HH} \approx$ 0.5 Hz, 1 H, =CH_2), 3.89 (s, 5 H, C_5H_5), 4.17 (m, 1 H, C_5H_3), 4.52 (dt, 1 H, C_5H_3), 4.64 (apparent t, 1 H, C_5H_3), 5.52 (dd, $^3J_{HH}$ = 13.4, 9.0 Hz, 1 H, =CH), 7.02−7.89 (m, 10 H, PPh_2). ^{13}C{^{1}H} NMR ($CDCl_3$): δ 64.61 (=CH_2), 67.51 (CH of C_5H_3), 69.12 (d, J_{PC} = 11 Hz, CH of C_5H_3), 70.27 (C_5H_5), 74.74 (d, J_{PC} = 4 Hz, CH of C_5H_3), 80.69 (d, $^1J_{PC}$ = 44 Hz, CP of C_5H_3), 80.96 (=CH), 102.03 (d, $^2J_{PC}$ = 35 Hz, CCH=CH_2 of C_5H_3), 128.16 (d, J_{PC} = 9 Hz), 128.41 (d, J_{PC} = 10 Hz), 128.81 (d, J_{PC} = 2 Hz), 129.81 (d, J_{PC} = 11 Hz), 130.87 (d, J_{PC} = 2 Hz), 134.26 (d, J_{PC} = 13 Hz) (6 × CH of PPh_2); 135.04 (d, $^1J_{PC}$ = 48 Hz), 140.62 (d, $^1J_{PC}$ = 43 Hz) (2 × C_{ipso} of PPh_2); 199.62 (d, $^2J_{PC}$ = 7 Hz), 203.57 (d, $^2J_{PC}$ = 32 Hz), 206.45 (d, $^2J_{PC}$ = 8 Hz), 210.27 (d, $^2J_{PC}$ = 5 Hz) (C≡O). ^{31}P{^{1}H} NMR ($CDCl_3$): δ +23.7 (s with ^{183}W satellites, $^1J_{WP}$ = 249 Hz). IR (Nujol): (ν/cm^{-1}): ν(C≡O) 2022 (vs), 1915−1930 (vs composite), 1874 (vs); 1308 (w), 1217 (m), 1183 (w), 1164 (w), 1096 (m), 1033 (m), 1000 (m), 917 (m), 857 (w), 830 (m), 815 (w), 747 (s), 692 (s), 602 (s), 570 (s), 512 (s), 502 (w), 484 (s), 763 (m), 438 (m). MS (EI): m/z (relative abundance) 682 (38, M$^{+\bullet}$), 664 (7, [M − CO]$^+$), 636 (1, [M − 2CO]$^+$), 608 (21, [M − 3CO]$^+$), 580 (65, [M − 4CO]$^+$), 502 (33), 500 (33), 474 (7), 445 (8), 424 (15), 396 (100, **1**$^{+\cdot}$), 369 (12), 331 (19), 288 (13), 275 (9),

252 (10), 196 (7), 133 (9), 121 (24, $[C_5H_5Fe]^+$), 108 (7), 78 (17), 56 (27, Fe^+). HR MS (EI): calcd for $C_{28}H_{21}{}^{56}FeO_4P^{184}W$, 692.0036; found 692.0057. $[\alpha]_D = -302$ ($c = 0.51$, $CHCl_3$). Anal. Calcd for $C_{28}H_{21}FeO_4PW$: C, 48.59; H, 3.06. Found: C, 48.55; H, 3.08.

Synthesis of Tungsten Carbonyl Complexes with (*Z*/*E*)-3. The reaction was performed similarly to the preparation of **9**. [W(cod)-$(CO)_4$] (82 mg, 0.20 mmol) and (*Z*/*E*)-**3** (84 mg, 0.20 mmol) in toluene (8 mL) were heated at reflux for 3 h. The reaction solution was filtered trough a short silica gel column, eluting with toluene. The yellow eluate was evaporated to give the crude product as an orange gummy residue with the characteristic smell of the liberated cyclooctadiene. This material was purified by column chromatography (silica gel, 10:1 hexane−diethyl ether). The first yellow band containing mostly impurities was discarded (ca. 15 mg). The second, major yellow band was evaporated to give and yellow-orange foam (ca. 120 mg), which was dissolved in boiling heptane (5 mL). The solution was treated with a little charcoal and filtered while hot and allowed to crystallize at 0 °C. The separated crystalline product was washed with pentane and dried under vacuum. Yield: 62 mg (44%), rusty brown crystalline solid. The product is a mixture of (*Z*)-**10** and (*E*)-**10** isomers in ca. 5:1 ratio.

MS (EI): *m*/*z* (relative abundance) 706 (23, $M^{+\bullet}$), 678 (10, $[M - CO]^+$), 650 (3, $[M - 2CO]^+$), 622 (15, $[M - 3CO]^+$), 594 (37, $[M - 4CO]^+$), 514 (13), 438 (15), 490 (11), 410 (100, $\mathbf{3}^{+\bullet}$), 395 (19, $[\mathbf{3} - Me]^+$), 183 (14), 121 (30, $[C_5H_5Fe]^+$). HR MS (EI): calcd for $C_{29}H_{23}{}^{56}FeO_4P^{184}W$, 706.0193; found 706.0210.

NMR Data for Tetracarbonyl[(*Z*,S_p)-2-(diphenylphosphino-κP)-1-(η(1,2)-prop-1-en-1-yl)ferrocene]tungsten(0), (*Z*)-10. ^{1}H NMR ($CDCl_3$): δ 1.71 (dd, $^3J_{HH} = 6.2$, $J_{PH} = 1.0$ Hz, 3 H, Me), 3.87 (s, 5 H, C_5H_5), 4.36 (dt, 1 H, C_5H_3), 4.43 (dt, 1 H, C_5H_3), 4.73 (t, 1 H, C_5H_3), 4.90 (ddq, $^3J_{HH} = 9.4$ Hz, $J_{PH} \approx 0.5$, $^3J_{HH} = 6.2$ Hz, 1 H, CH=C*H*Me), 5.77 (br "dd", $^3J_{HH} = 9.4$ Hz, $J_{PH} \approx 1.0$ Hz, 1 H, C*H*=CHMe), 7.10−7.92 (m, 10 H, PPh_2). $^{13}C\{^1H\}$ NMR ($CDCl_3$): δ 16.90 (Me), 68.75, 68.99 (d, $J_{PC} = 12$ Hz) (2 × CH of C_5H_3); 70.41 (C_5H_5), 75.29 (d, $J_{PC} = 4$ Hz, CH of C_5H_3), 84.58 (*C*H=CHMe), 86.94 (d, $^1J_{PC} = 43$ Hz, CP of C_5H_3), 89.49 (CH=*C*HMe), 97.17 (d, $^2J_{PC} = 37$ Hz, *C*CH=CH of C_5H_3), 128.08 (d, $J_{PC} = 10$ Hz), 128.40 (d, $J_{PC} = 10$ Hz), 128.71 (d, $J_{PC} = 2$ Hz), 130.27 (d, $J_{PC} = 11$ Hz), 130.63 (d, $J_{PC} = 2$ Hz), 134.04 (d, $J_{PC} = 13$ Hz) (6 × CH of PPh_2); 136.64 (d, $^1J_{PC} = 47$ Hz), 139.80 (d, $^1J_{PC} = 44$ Hz) (2 × C_{ipso} of PPh_2); 201.12 (d, $^1J_{PC} = 7$ Hz), 204.83 (d, $^1J_{PC} = 29$ Hz), 205.63 (d, $^1J_{PC} = 8$ Hz), 209.83 (d, $^1J_{PC} = 5$ Hz) (4 × C≡O). $^{31}P\{^1H\}$ NMR ($CDCl_3$): δ +24.9 (s with ^{183}W satellites, $^1J_{WP} = 249$ Hz).

NMR Data for Tetracarbonyl[(*E*,S_p)-2-(diphenylphosphino-κP)-1-(η(1,2)-prop-1-en-1-yl)ferrocene]tungsten(0), (*E*)-10. $^{31}P\{^1H\}$ NMR ($CDCl_3$): δ +24.4 (s, ^{183}W satellites not read).

Preparation of Tungsten Carbonyl Complexes with (*E*)-4. [W(cod)$(CO)_4$] (82 mg, 0.20 mmol) and (*E*)-**4** (95 mg, 0.20 mmol) in toluene (8 mL) were heated at 100 °C (temperature in the bath) in the dark for 2 h. The reaction mixture was cooled to room temperature and filtered through a short silica gel column (elution with toluene). The orange eluate was evaporated under reduced pressure to give an orange-red oil (ca. 124 mg, smell of the liberated cyclooctadiene was clearly detectable), which was subsequently purified by column chromatography on silica gel. Eluting with 10:1 hexane−diethyl ether gave three fractions, followed by a small band due to a brown material (probably decomposition products). The first, very minor, yellow band was discarded. The second yellow band was evaporated to give an orange glassy solid (65 mg) whose subsequent crystallization from heptane (3 mL) afforded analytically pure (*E*)-**11** as well-developed, dark ruby red crystals, which were isolated by suction (46 mg, 28%). Finally, evaporation of the third yellow fraction gave compound (*E*)-**12** as a bright orange amorphous solid (ca. 35 mg, 23%). Note: the product distribution can be shifted in favor of the chelate complex by increasing the reaction temperature and time. For instance, heating the same educt mixture at reflux temperature for 3 h gave a mixture containing (*E*)-**12** (ca. 90%) and (*E*)-**11** (ca. 10%**)**. Chromatographic purification of the product mixture was rather tedious due to similar retention characteristics of its components.

Analytical Data for Pentacarbonyl[(*E*,S_p)-2-(diphenylphosphino-κP)-1-(2-phenylethen-1-yl)ferrocene]tungsten(0) ((*E*)-11). ^{1}H NMR ($CDCl_3$): δ 4.28 (s, 5 H, C_5H_5), 4.41 (m, 1 H, C_5H_3), 4.66 (m, 1 H, C_5H_3), 4.98 (m, 1 H, C_5H_3), 6.30 and 6.61 (2 × d, $^3J_{HH} = 16.0$ Hz, CH=CH), 6.99−7.81 (m, 15 H, Ph and PPh_2). $^{13}C\{^1H\}$ NMR ($CDCl_3$): δ 69.42 (d, $J_{PC} = 4$ Hz), 70.48 (d, $J_{PC} = 9$ Hz) (2 × CH of C_5H_3); 71.12 (C_5H_5), 77.59 (d, $^1J_{PC} = 40$ Hz, CP of C_5H_3), 77.79 (d, $J_{PC} = 18$ Hz, CH of C_5H_3), 86.77 (d, $^2J_{PC} = 4$ Hz, *C*CH=CH of C_5H_3), 124.74 (d, $J_{PC} \approx 1$ Hz, *C*H=CHPh; correlation with δ_H 6.30), 125.94, 127.13 (2 × CH of Ph); 128.17 (d, $J_{PC} = 10$ Hz, CH of PPh_2), 128.32 (CH=*C*HPh; correlation with δ_H 6.61), 128.36 (d, $J_{PC} = 10$ Hz, CH of PPh_2), 128.50 (CH of Ph), 129.76 (d, $J_{PC} = 2$ Hz), 130.36 (d, $J_{PC} = 2$ Hz), 132.08 (d, $J_{PC} = 12$ Hz), 133.27 (d, $J_{PC} = 12$ Hz) (4 × CH of PPh_2); 135.82 (d, $^1J_{PC} = 41$ Hz), 136.51 (d, $^1J_{PC} = 43$ Hz) (2 × C_{ipso} of PPh_2); 137.13 (C_{ipso} of Ph), 197.73 (d, $^2J_{PC} = 7$ Hz, ^{183}W satellites, $^1J_{WC} = 126$ Hz, C≡O *cis*-P), 198.97 (d, $^2J_{PC} = 22$ Hz, ^{183}W satellites not detected, C≡O *trans*-P). $^{31}P\{^1H\}$ NMR ($CDCl_3$): δ +11.1 (s with ^{183}W satellites, $^1J_{WP} = 246$ Hz). IR (Nujol) (ν/cm^{-1}): ν(C≡O) 2069 (vs), 1989 (m), ca. 1880−1955 (vs, br composite); 1311 (w), 1248 (w), 1159 (m), 1149 (m), 1108 (m), 1093 (m), 1000 (m), 984 (w), 957 (m), 824 (m), 762 (m), 751 (s), 745 (s), 707 (m), 696 (s), 598 (vs), 579 (vs), 562 (m), 510 (m), 485 (s), 466 (s), 452 (m). HR MS (FAB): calcd for $C_{35}H_{26}{}^{56}FeO_5P^{184}W$ ($[M + H]^+$), 797.0377; found 768.0352. Anal. Calcd for $C_{35}H_{25}FeO_5PW$: C, 52.79; H, 3.16. Found: C, 52.57; H, 3.14.

Analytical Data for Tetracarbonyl[(*E*,S_p)-2-(diphenylphosphino-κP)-1-(η(1,2)-2-phenylethen-1-yl)ferrocene]tungsten(0) ((*E*)-12). ^{1}H NMR ($CDCl_3$): δ 3.93 (s, 5 H, C_5H_5), 4.23 (br s, 1 H, C_5H_3), 4.52 (m, 1 H, C_5H_3), 4.66 (m, 1 H, C_5H_3), 4.79 (dd, $^3J_{HH} = 13.1$, $^4J_{PH} = 1.2$ Hz, 1 H, C*H*=CHPh), 5.89 (dd, $^3J_{HH} = 13.1$, $^5J_{PH} = 0.9$ Hz, 1 H, CH=C*H*Ph), 7.06−7.85 (m 15 H, Ph and PPh_2). $^{13}C\{^1H\}$ NMR ($CDCl_3$): δ 67.54, 69.39 (d, $J_{PC} = 12$ Hz) (2 × CH of C_5H_3); 70.32 (C_5H_5), 74.91 (d, $J_{PC} = 4$ Hz, CH of C_5H_3), 75.38 (CH=*C*HPh), 80.20 (d, $^1J_{PC} = 44$ Hz, CP of C_5H_3), 86.53 (*C*H=CHPh), 103.15 (d, $^2J_{PC} = 38$ Hz, *C*CH=CH of C_5H_3), 125.10, 127.01 (2 × CH of Ph); 128.30 (d, $J_{PC} = 9$ Hz, CH of PPh_2), 128.37 (CH of Ph), 128.42 (d, $J_{PC} = 12$ Hz), 128.92 (d, $J_{PC} = 1$ Hz), 129.89 (d, $J_{PC} = 11$ Hz), 130.90 (d, $J_{PC} = 2$ Hz), 134.18 (d, $J_{PC} = 13$ Hz) (5 × CH of PPh_2); 134.98 (d, $^1J_{PC} = 48$ Hz), 140.70 (d, $^1J_{PC} = 43$ Hz) (2 × C_{ipso} of PPh_2); 141.19 (C_{ipso} of Ph), 201.79 (d, $^2J_{PC} = 5$ Hz, ^{183}W satellites, $^1J_{WC} = 124$ Hz), 203.14 (d, $^2J_{PC} = 33$ Hz, ^{183}W satellites, $^1J_{WC} = 154$ Hz), 206.51 (d, $^2J_{PC} = 8$ Hz, ^{183}W satellites, $^1J_{WC} = 123$ Hz), 212.47 (d, $^2J_{PC} = 5$ Hz, ^{183}W satellites, $^1J_{WC} = 151$ Hz) (4 × C≡O). $^{31}P\{^1H\}$ NMR ($CDCl_3$): δ +24.9 (s with ^{183}W satellites, $^1J_{WP} = 293$ Hz). IR (Nujol) (ν/cm^{-1}): ν(C≡O) 2022 (vs), 1870−1945 (vs, br composite); 1306 (w), 1253 (m), 1215 (m), 1158 (m), 1098 (s), 1076 (m), 1027 (m), 1001 (m), 826 (s), 749 (s), 739 (s), 693 (vs), 601 (s), 576 (s), 520 (vs), 506 (m), 484 (s), 462 (s). MS (EI): *m*/*z* (relative abundance) 768 (3, $M^{+\bullet}$), 740 (2, $[M - CO]^+$), 712 (5, $[M - 2CO]^+$), 686 (3, $[M - 3CO]^+$), 658 (3, $[M - 4CO]^+$), 576 (3), 438 (15), 472 (100, $\mathbf{4}^{+\bullet}$). HR MS (EI): calcd for $C_{34}H_{25}{}^{56}FeO_4P^{184}W$, 768.0349; found, 768.0355.

X-ray Crystallography. Single crystals suitable for X-ray diffraction analysis were selected from the reaction batch (**1**, red prism,

Table 5. Crystallographic Data and Data Collection and Structure Refinement Parameters for **1**, **2**, **8**, **9**, and (*E*)-**11**

param	**1**	**2**	**8**	**9**	(*E*)-**11**
formula	$C_{23}H_{19}FeOP$	$C_{24}H_{21}FeP$	$C_{33}H_{33}ClFeNO_4PPd$	$C_{28}H_{21}FeO_4PW$	$C_{35}H_{25}FeO_5PW$
M_r (g mol^{-1})	398.20	396.23	736.27	652.12	796.22
cryst system	monoclinic	orthorhombic	monoclinic	orthorhombic	orthorhombic
space group	$P2_1$ (No. 4)	$P2_12_12_1$ (No. 19)	$P2_1$ (No. 4)	$P2_12_12_1$ (No. 19)	$P2_12_12_1$ (No. 19)
a (Å)	8.4927(1)	10.5452(2)	9.0782(2)	10.0170(1)	12.915(1)
b (Å)	17.2736(2)	12.9788(2)	14.3355(2)	11.4879(2)	13.742(2)
c (Å)	13.0060(1)	13.8939(2)	12.4391(2)	21.2688(4)	34.841(1)
β (deg)	103.6854(6)		105.508(1)		
V (Å^3)	1853.81(3)	1901.58(5)	1559.89(5)	2447.49(7)	6184(1)
Z	4	4	2	4	8
D (g mL^{-1})	1.427	1.384	1.568	1.878	1.711
μ(Mo Kα) (mm^{-1})	0.908	0.881	1.216	5.388	4.280
T^a	0.710−0.886	[f]	0.705−0.939	0.495−0.755	0.349−0.555
reflcn tot.	54 311[e]	30 254[e]	27 206[e]	34 771[e]	83 405[g]
unique/obsd[b] reflcns	8482/8257	4345/4192	7035/6630	5595/5318	12 848/10 627
R_{int} (%)[c]	3.58	3.80	3.64	5.45	4.13
no. of params	434	235	393	328	707
R (obsd reflcns) (%)[d]	2.43	2.22	2.65	2.27	2.65
R, wR (all data) (%)[d]	2.56, 5.94	2.38, 5.32	3.05, 5.76	2.58, 4.95	3.99, 4.76
Flack's param	−0.019(7)	0.00(1)	−0.03(1)	−0.019(6)	−0.022(4)
$\Delta\rho$ (e Å^{-3})	0.52, −0.41	0.23, −0.25	0.56, −0.49	1.09, −1.05	1.18, −0.64
CCDC deposition no.	604808	604809	604810	604811	604812

[a] The range of transmission coefficients. [b] Reflections with $I_o > 2\sigma(I_o)$. [c] $R_{int} = \sum|F_o^2 - F_o^2(\text{mean})|/\sum F_o^2$, where F_o^2(mean) is the average intensity for symmetry-equivalent diffractions. [d] $R = \sum||F_o| - |F_c||/\sum|F_o|$, $wR = [\sum\{w(F_o^2 - F_c^2)^2\}/\sum w(F_o^2)^2]^{1/2}$. [e] $2\theta \le 55°$. [f] Not corrected. [g] $2\theta \le 53°$.

0.20 × 0.30 × 0.50 mm^3) or were grown by crystallization from hot heptane (**2**, red-brown prism, 0.20 × 0.25 × 0.38 mm^3; **9**, orange bar, 0.06 × 0.13 × 0.30 mm^3; (*E*)-**11**, deep red fragment, 0.06 × 0.13 × 0.23 mm^3) or from dichloromethane−diethyl ether (**8**, rusty brown plate; 0.05 × 0.15 × 0.38 mm^3). Full-set diffraction data ($\pm h \pm k \pm l$) were collected on Nonius KappaCCD (**1**, **2**, **8**, **9**) and Oxford KM4 CCD ((*E*)-**11**) diffractometers equipped with Cryostream Cooler (Oxford Cryosystems) and Oxford Cryojet (Oxford Instruments), respectively, at 150(2) K using graphite-monochromatized Mo Kα radiation (λ = 0.710 73 Å). The data for **8**, **9**, and (*E*)-**11** were corrected for absorption (**8** and **9**, a Gaussian method based on the indexed crystal shape; (*E*)-**11**, an analytical method). Relevant crystallographic data are given in Table 5.

The structures were solved by direct methods (SIR97[54]) and refined by weighted full-matrix least squares on F^2 (SHELXL97[55]). Final geometric calculations were carried out with a recent version of Platon program.[56] All non-hydrogen atoms were freely refined with anisotropic thermal motion parameters. Hydrogen atoms were included in the calculated positions and refined using the "riding" model.

Crystallographic data for all structures excluding the structure factors have been deposited with the Cambridge Crystallographic Data Centre (see the Supporting Information paragraph).

Acknowledgment. Financial support for this study was provided by the Czech Science Foundation (Grant No. GA CR 203/05/0276). We thank Professor Jiří Ludvík for providing access to the electrochemical apparatus and Helena Dlouhá for recording CD spectra.

Supporting Information Available: Complete crystallographic data (excluding the structure factors) as CIF files and alternative views of (*Z*/*E*)-**10** (Figures S1 and S2). This material is available free of charge via the Internet at http://pubs.acs.org. Alternatively, the crystallographic data can be obtained via www.ccdc.cam.ac.uk/conts/retrieving.html or from the Cambridge Crystallographic Data Center, 12 Union Road, Cambridge CB21EZ, U.K. (fax, +44 1223-336-033; e-mail, deposit@ccdc.cam.ac.uk). The deposition numbers are given in Table 5.

IC061278G

(54) Altomare, A.; Burla, M. C.; Camalli, M.; Cascarano, G. L.; Giacovazzo, C.; Guagliardi, A.; Moliterni, A. G. G.; Polidori, G.; Spagna, R. *J. Appl. Crystallogr.* **1999**, *32*, 115−119.

(55) Sheldrick, G. M. *SHELXL97. Program for Crystal Structure Refinement from Diffraction Data*; University of Göttingen: Göttingen, Germany, 1997.

(56) Spek, A. L. *Platon-A multipurpose crystallographic tool.* Available via the Internet at http://www.cryst.chem.uu.nl/platon/.